MATHEMATICAL ENGINEERING TECHNICAL REPORTS

Using Zolotarev's Rational Approximation for Computing the Polar, Symmetric Eigenvalue, and Singular Value Decompositions

Yuji NAKATSUKASA and Roland W. FREUND

METR 2014–35 December 2014

DEPARTMENT OF MATHEMATICAL INFORMATICS
GRADUATE SCHOOL OF INFORMATION SCIENCE AND TECHNOLOGY
THE UNIVERSITY OF TOKYO
BUNKYO-KU, TOKYO 113-8656, JAPAN

WWW page: http://www.keisu.t.u-tokyo.ac.jp/research/techrep/index.html

USING ZOLOTAREV'S RATIONAL APPROXIMATION FOR COMPUTING THE POLAR, SYMMETRIC EIGENVALUE, AND SINGULAR VALUE DECOMPOSITIONS

YUJI NAKATSUKASA* AND ROLAND W. FREUND†

Abstract. Conventional algorithms for basic matrix decompositions, such as the symmetric eigenvalue decomposition and the singular value decomposition (SVD), are suboptimal in view of recent trends in computer architectures, which require minimizing communication together with arithmetic costs. Spectral divide-and-conquer algorithms can achieve both requirements, which recursively decouple the problem into two smaller subproblems. One natural way to execute spectral divide-and-conquer is via the polar decomposition. For computing the polar decomposition, the scaled Newton and QDWH iterations are two of the most popular algorithms, as they are backward stable and converge in at most nine and six iterations, respectively. Following this framework, we propose a new higher-order variant of the QDWH iteration. The key idea of this algorithm comes from approximation theory: we use the best rational approximant for the scalar sign function due to Zolotarev in 1877, which lets the algorithm converge in just *two* iterations, with the whopping rate of convergence *seventeen.* The algorithm employs a high-degree Zolotarev function (best rational approximant) obtained by composing low-degree Zolotarev functions, an extraordinary property enjoyed by the sign function. The resulting algorithms for the polar, symmetric eigenvalue, and singular value decompositions have higher arithmetic costs than the QDWH-based algorithms but are better-suited for parallel computing, and exhibit excellent numerical backward stability.

Key words. Zolotarev, rational approximation, symmetric eigenvalue problem, SVD, polar decomposition, communication-minimizing algorithms

AMS subject classifications. 15A23, 65F15, 65F30, 65G50

1. Introduction.

The eigenvalue decomposition $A = V\Lambda V^*$ of symmetric (or Hermitian) matrices and the singular value decomposition (SVD) $A = U\Sigma V^*$ of general matrices are two of the most fundamental matrix decompositions with wide areas of applications [4, 15]. There has been much recent progress on designing algorithms that reduce communication in addition to the arithmetic cost [6], so that they are well-suited for parallel computing. Unfortunately, the standard algorithms based on initial reduction to condensed form [15] do not minimize communication in a naive implementation [5]. Recent attempts [7] modify the reduction stage for the symmetric eigendecomposition to reduce communication, but its implementation details are unavailable, and involve a significant amount of tuning that depends on the architecture.

A completely different approach is pursued in [30, Ch. 3,4], [33], which propose backward stable algorithms based on spectral divide-and-conquer for the two decompositions that can be implemented in a communication-minimizing manner using only widely available and highly optimized matrix operations such as matrix multiplication and QR and Cholesky decompositions, while requiring arithmetic operation costs within a factor 3 of those for the most efficient existing algorithms. We outline the algorithms below.

- Symmetric eigendecomposition $A = VDV^*$: Compute the polar decomposition $A - \sigma I = U_pH$, where $\sigma \approx \text{median}(\text{eig}(A))$. Obtain orthogonal

*Department of Mathematical Informatics, University of Tokyo, Tokyo 113-8656, Japan (nakatsukasa@mist.i.u-tokyo.ac.jp). Supported by JSPS Grants-in-Aid for Scientific Research No. 26870149. Part of this work was done while this author was a postdoc at the University of Manchester and supported by EPSRC grant EP/I005293/1.

†Department of Mathematics, University of California, Davis, CA 95616 (freund@math.ucdavis.edu)

$V = [V_1\ V_2]$ such that $\frac{1}{2}(U_p + I) = V_1 V_1^*$. Form $[V_1\ V_2]^* A [V_1\ V_2] = \begin{bmatrix} A_1 & E^* \\ E & A_2 \end{bmatrix}$ and verify that E is negligible. Repeat the process with $A \leftarrow A_1$ and $A \leftarrow A_2$ until A is diagonalized.

- SVD: Compute the polar decomposition $A = U_p H$. Obtain the symmetric eigendecomposition $H = V \Sigma V^*$ by the above algorithm. Then $A = (U_p V) \Sigma V^* = U \Sigma V^*$ is the SVD.

We stress that the above algorithms both rely heavily on the computation of the polar decomposition $A = U_p H$; see Section 2 for details on the polar decomposition. The arithmetic cost for the symmetric eigendecomposition is about $1 + \frac{1}{3}$ times that of computing $A = U_p H$, and about $2 + \frac{1}{3}$ for the SVD. Furthermore, it is shown in [30] that if the polar decomposition and an orthonormal column space V_1 of an orthogonal projection matrix $V_1 V_1^*$ are obtained in a backward stable manner throughout the spectral divide-and-conquer process, then the computed symmetric eigendecomposition and the SVD are also backward stable.

The approach in [30, 33] for computing the polar decomposition is to use the QDWH (QR-based dynamically weighted Halley) iteration developed in [31]. The analysis in [32] proves its backward stability when pivoting is employed, and in practice even without pivoting QDWH shows excellent backward stability. Therefore the resulting algorithms for the eigendecomposition (QDWH-eig) and the SVD (QDWH-SVD) are numerically backward stable, and in fact they typically give better backward errors than standard algorithms [33]. Since QDWH uses only matrix multiplication and QR and Cholesky factorizations as building blocks, the resulting algorithms can be implemented in a communication-minimizing manner in the asymptotic sense [6]. The dominant cost of one QDWH iteration is in performing the QR factorization of matrices of the form $\begin{bmatrix} X \\ cI \end{bmatrix}$ for a scalar c. QDWH requires at most six iterations to converge for any practical matrix in double precision arithmetic [31].

However, the experiments in [33] indicate that the QDWH-based algorithms are still considerably slower on a sequential machine (by a factor between 2 and 4) than the fastest standard algorithm. Although the relative performance is expected to be better on parallel systems, further improvements to the algorithm itself are therefore much desired. Since the spectral divide-and-conquer algorithms use the polar decomposition as fundamental building blocks, the design of an improved algorithm for $A = U_p H$ would directly lead to improved spectral divide-and-conquer algorithms for the symmetric eigendecomposition and the SVD.

The main contribution of this work is the design of Zolo-pd, an algorithm for the polar decomposition that requires just *two* iterations[1] for convergence in double precision for any matrix A with $\kappa_2(A) \le 10^{16}$. The crucial observation is that the mapping function on the singular values used by the QDWH iteration is exactly the type-$(3,2)$ best rational approximation of the scalar sign function. Then a natural idea is to consider type-$(2r+1, 2r)$ best rational approximations for general $r \ge 1$. The explicit solution of this rational approximation problem was given by Zolotarev in 1877. We show that the type-$((2r+1)^k, (2r+1)^k - 1)$ best approximation can be expressed as a composition of the form $R_k(\cdots(R_1(x))\cdots)$, where each R_i is a rational function of type $(2r+1, 2r)$. Based on this observation, we derive the Zolo-pd algorithm that requires only k iterations to apply the type-$((2r+1)^k, (2r+1)^k - 1)$ best

[1]The two-step convergence of Zolo-pd suggests that perhaps it should be regarded as a direct rather than an iterative algorithm: even though it is known [13, 14] that Abel's impossibility theorem implies that the exact polar decomposition cannot be computed in a finite number of arithmetic operations, an approximation correct to $\mathcal{O}(10^{-16})$ can be obtained.

approximation. The high-order rational approximations to the sign function $\mathrm{sign}(x)$ are so powerful that a type-$(m+1, m)$ best approximant on the interval $[10^{-15}, 1]$ with $m \geq 280$ has accuracy $\mathcal{O}(u)$ where $u \approx 1.1 \times 10^{-16}$ is the unit roundoff in IEEE double precision arithmetic. Since taking $r = 8$ yields a type $(289, 288)$ approximant with $k = 2$, this means just *two* iterations is enough to obtain $\mathcal{O}(u)$ accuracy on $[10^{-15}, 1]$. This precisely means Zolo-pd converges in two steps as a matrix iteration. The algorithm is still iterative (it has to be), and the rate of convergence is as high as *seventeen*, which means one iteration reduces the error from ε to $\mathcal{O}(\varepsilon^{17})$. This is significantly higher than any other practical numerical algorithm that the authors are aware of. For example, the widely used Newton's method typically converges quadratically, i.e., its convergence rate is 2, and cubically convergent methods with rate 3 are often regarded as extremely fast; for example the QR algorithm for symmetric tridiagonal matrices [35] and QDWH.

It is often believed (and sometimes true) that higher-order iterations can cause numerical instability. However, with the help of a QR-based implementation Zolo-pd exhibits excellent numerical stability comparable to that of QDWH, leading to stable algorithms also for computing the symmetric eigendecomposition (Zolo-eig) and the SVD (Zolo-SVD). Their experimental backward stability and orthogonality measure are comparable to QDWH-eig and QDWH-SVD, and are notably better than those of standard algorithms.

Using the partial fraction form of the type $(2r+1, 2r)$ rational function, each iteration of Zolo-pd involves computing the QR factorization $\left[\begin{smallmatrix} X \\ c_j I \end{smallmatrix}\right] = QR$ for distinct values of c_j, $j = 1, \ldots, r (\leq 8)$. Just like the QDWH-based algorithms, the Zolo-based algorithms require only matrix multiplications and QR and Cholesky factorizations, hence minimizes communication. The arithmetic cost of the Zolo-based algorithms is higher than the QDWH-based ones (by a factor < 3), so on a serial implementation Zolo-pd is slower than QDWH; this is reflected in our MATLAB experiments. Fortunately, the r QR factorizations can be performed independently, in which case the runtime per iteration is expected to be roughly the same as QDWH. Then, due to the faster convergence, Zolo-pd can be faster than QDWH by a factor up to 3. Indeed, in a parallel implementation, the arithmetic cost of Zolo-SVD along the critical path is less than that of the standard algorithms based on reduction to bidiagonal form. Zolo-based algorithms therefore have ideal properties for parallel computing, and our preliminary MATLAB experiments suggest that if properly parallelized, our algorithms can outperform standard algorithms in both speed and accuracy. This paper focuses on the mathematical foundations of the algorithm, and optimizing the performance on massively parallel systems is left as future work.

The structure of this paper is as follows. In Section 2 we revisit the QDWH iteration from the viewpoint of approximation theory. In Section 3 we develop its higher-order variant, in which we show the composed Zolotarev functions is another Zolotarev function. Section 4 discusses detailed algorithmic implementation issues such as a stable and parallelizable evaluation of the iteration. We then summarize the Zolo-based algorithms and compare them with other standard algorithms in Section 5. Numerical experiments with a sequential implementation are presented in Section 6.

Notation: $\sigma_1(A) \geq \cdots \geq \sigma_n(A)$ are the singular values of a rectangular matrix $A \in \mathbb{C}^{m\times n}$ with $m \geq n$, and $\sigma_{\max}(A) = \sigma_1(A)$ and $\sigma_{\min}(A) = \sigma_n(A)$. $\|A\|_2 = \sigma_{\max}(A)$ denotes the spectral norm and $\|A\|_F = \sqrt{\sum_{i,j} A_{ij}^2}$ is the Frobenius norm. $\lambda_i(A)$ denotes the ith largest eigenvalue of a Hermitian matrix A. $\kappa_2(A) = \sigma_{\max}(A)/\sigma_{\min}(A)$ is the condition number of A. To avoid confusion between the unitary polar factor and the singular value decomposition (SVD) of A, we always use subscripts U_p to denote the unitary polar factor, while U denotes the matrix of left singular vectors. Hence for example $A = U_pH = U\Sigma V^*$. We denote by $\mathcal{P}_r$ the set of all polynomials P with real coefficients of degree at most r and by $\mathcal{R}_{r,s}$ the set of all rational functions $R = \frac{P}{Q}$ where $P \in \mathcal{P}_r$, $Q \in \mathcal{P}_s$. We say that a rational function R is of type (r, s) if $R \in \mathcal{R}_{r,s}$.

We develop algorithms for complex matrices $A \in \mathbb{C}^{m\times n}$, but for $A \in \mathbb{R}^{m\times n}$ all the operations can be carried out using real arithmetic only. We assume the use of IEEE double precision arithmetic, in which the unit roundoff $u = 2^{-53} \approx 1.1 \times 10^{-16}$, but minor modifications extends the discussion to higher (or lower) precision arithmetic.

2. The QDWH algorithm as a rational approximation to $\mathrm{sign}(x)$**.** Any rectangular matrix $A \in \mathbb{R}^{m\times n}$ $(m \geq n)$ has a polar decomposition [20, Thm. 8.1], [22, Sec. 7.3]

$$A = U_pH, \tag{2.1}$$

where U_p has orthonormal columns and H is symmetric positive semidefinite. The polar decomposition (2.1) is unique if A has full column rank, which we assume in most of the paper (see Section 5.4 for the rank-deficient case).

QDWH [31] computes the unitary polar factor U_p of a full-rank matrix A as the limit of the sequence X_k defined by

$$X_{k+1} = X_k(a_kI + b_kX_k^*X_k)(I + c_kX_k^*X_k)^{-1}, \qquad X_0 = A/\alpha. \tag{2.2}$$

Here, $\alpha > 0$ is an estimate of $\|A\|_2$ such that $\alpha \gtrsim \|A\|_2$. Setting $a_k = 3$, $b_k = 1$, $c_k = 3$ gives the Halley iteration, which is the cubically convergent member of the family of principal Padé iterations [20, Sec. 8.5]. The iterates (2.2) preserve the singular vectors while mapping the singular values by a rational function $R_k(\cdots R_2(R_1(x))\cdots)$, that is, $X_k = U\Sigma_kV^*$, where $\Sigma_k = R_k(\cdots R_2(R_1(\Sigma))\cdots)$ is the diagonal matrix with ith diagonal $R_k(\cdots R_2(R_1(\sigma_i))\cdots)$; equivalently $R(\Sigma)$ denotes the matrix function in the classical sense [20]. The choice of the rational functions $R_k(x)$ is of crucial importance in this paper, and in QDWH $R_k(x) = x\frac{a_k+b_kx^2}{1+c_kx^2}$, in which the parameters a_k, b_k, c_k are chosen dynamically to speed up the convergence. They are computed by $a_k = h(\ell_k)$, $b_k = (a_k - 1)^2/4$, $c_k = a_k + b_k - 1$, where $h(\ell) = \sqrt{1+\gamma} + \frac{1}{2}\big(8 - 4\gamma + 8(2-\ell^2)/(\ell^2\sqrt{1+\gamma})\big)^{1/2}$, $\gamma = \big(4(1-\ell^2)/\ell^4\big)^{1/3}$. Here, ℓ_k is a lower bound for the smallest singular value of X_k, which is computed from the recurrence $\ell_k = \ell_{k-1}(a_{k-1} + b_{k-1}\ell_{k-1}^2)/(1 + c_{k-1}\ell_{k-1}^2)$ for $k \geq 1$. Note that all the parameters are available for free (without any matrix computations) for all $k \geq 0$ once we have estimates $\alpha \gtrsim \|A\|_2$ and $\ell_0 \lesssim \sigma_{\min}(X_0)$, obtained for example via a condition number estimator.

With such parameters the iteration (2.2) is cubically convergent and needs at most six iterations for convergence to U_p with the tolerance u for any matrix A with $\kappa_2(A) \leq u^{-1}$, that is, $\|X_6 - U_p\|_2 = \mathcal{O}(u)$.

The iteration (2.2) has a mathematically equivalent QR-based implementation, which is numerically more stable (this is the actual QDWH iteration):

$$\begin{bmatrix} \sqrt{c_k}X_k \\ I \end{bmatrix} = \begin{bmatrix} Q_1 \\ Q_2 \end{bmatrix} R, \quad X_{k+1} = \frac{b_k}{c_k}X_k + \frac{1}{\sqrt{c_k}}\left(a_k - \frac{b_k}{c_k}\right)Q_1Q_2^*, \quad k \geq 0. \tag{2.3a}$$

Once the computed polar factor $\widehat{U}_p$ is obtained, we compute the symmetric polar factor $\widehat{H}$ by $\widehat{H} = \frac{1}{2}(\widehat{U}_p^*A + (\widehat{U}_p^*A)^*)$ [20, Sec. 8.8].

2.1. QDWH mapping function seen as the best type-$(3,2)$ approximation. The QDWH parameters a,b,c in (2.2) are chosen so that the interval $[\ell,1]$ (in which all the singular values of X lie) is mapped as close as possible to the point 1 by the type $(3,2)$ rational function $R(x)=x\frac{a+bx^2}{1+cx^2}\in\mathcal{R}_{3,2}$. In [31] they are obtained as the solution for the rational max-min optimization problem

$$\max_{a,b,c}\min_{\ell\le x\le 1} x\frac{a+bx^2}{1+cx^2}, \tag{2.4}$$

subject to the constraint $x\frac{a+bx^2}{1+cx^2}\le 1$ on $[0,1]$. The solution a,b,c results in the function that takes exactly one local maximum $R(x_M)$ and minimum $R(x_m)$ on $[\ell,1]$ such that $\ell\le x_M\le x_m\le 1$, and $R(x_M)=R(1)=1$, $R(x_m)=R(\ell)$. The function $R(x)$ maps the interval $[\ell,1]$ to $[R(\ell),1]$. Figure 2.1 is a plot of $R(x)$ for the case $\ell=0.01$.

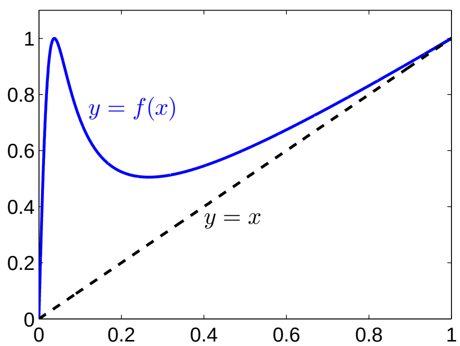

FIG. 2.1. *Plot of $R(x)$ for the QDWH iteration when $\ell=0.01$.*

Note that defining $\tau=(R(1)+R(\ell))/2$, the function $R(x)-\tau$ exhibits an *equioscillation* behavior on $[\ell,1]$ with four extreme points, which is easily seen to be the largest possible by counting the number of critical points that an odd function $R(x)\in\mathcal{R}_{3,2}$ can have. This is known as the equioscillation property of best rational approximants [39], and implies optimality of $\frac{R(x)}{\tau}$ as an approximation to the sign function on $[-1,-\ell]\cup[\ell,1]$; we give more details in Section 3.3. This means the parameters in the QDWH iteration can also be determined by finding the best type-$(3,2)$ rational approximation to the sign function in the infinity norm (called a Zolotarev function), then scaling so that $\max_{0\le x\le 1}R(x)=1$.

QDWH runs this process iteratively, and the resulting function R_k in the kth QDWH iteration maps the interval $[\ell_{k-1},1]$ to $[\ell_k,1]=R_k([\ell_{k-1},1])$ with $|1-\ell_k|\ll|1-\ell_{k-1}|$. Then the next QDWH iteration forms $R_{k+1}(x)$ defined by the parameters $(a_{k+1},b_{k+1},c_{k+1})\neq(a_k,b_k,c_k)$, so that $[\ell_{k+1},1]=R_{k+1}([\ell_k,1])=R_{k+1}(R_k([\ell_{k-1},1]))=R_{k+1}(R_k\circ\cdots R_1([\ell_0,1]))$ with ℓ_{k+1} as close as possible to the point 1. The QDWH iteration therefore attempts to map the interval $[\ell_0,1]=[\sigma_{\min}(X_0),1]$ as close as possible to 1 by the composed rational function $G_k(x)=R_k(R_{k-1}(\cdots R_2(R_1(x))\cdots)$. As we shall see below, after six QDWH iterations, $G_6(x)$ is in fact the *best* rational approximation to $\mathrm{sign}(x)$ (i.e., a Zolotarev function) of type-$(3^6,3^6-1)$ on $[-1,-\ell]\cup[\ell,1]$, which is so powerful as an approximant that $G_6([\ell,1]))\subseteq[1-u,1]$ for any ℓ such that $u<\ell\le 1$. Since $X_6=UG_6(\varSigma)V^*$ where $A=U\varSigma V^*$ is the SVD, this means $\|X_6-U_p\|_2=\|G_6([\ell,1]))-I\|_2\le u$, explaining why QDWH converges in six steps.

3. Zolotarev's rational approximations of the sign function. In light of the above observation, a natural idea is to consider approximations $R \in \mathcal{R}_{2r+1,2r}$ of the sign function $\mathrm{sign}(x)$ for general $r \geq 1$, with the goal to map all the singular values to 1. Since $\mathrm{sign}(x)$ is an odd function, the optimal approximant in $\mathcal{R}_{2r+1,2r}$ has the form $R(x) \equiv x\frac{P(x^2)}{Q(x^2)}$, where $P, Q \in \mathcal{P}_r$. As in the QDWH case (2.4), one way to obtain P and Q is to solve the max-min problem

$$\max_{P,Q\in\mathcal{P}_r} \min_{\ell\leq x\leq 1} x\frac{P(x^2)}{Q(x^2)} \tag{3.1}$$

subject to the constraint $x\frac{P(x^2)}{Q(x^2)} \leq 1$ on $[0,1]$. However, solving (3.1) via extending the approach in [31] for $r = 1$ to $r \geq 2$ seems highly nontrivial.

3.1. Zolotarev functions. Fortunately, the max-min problem (3.1) is equivalent to one of the classical rational approximation problems that Zolotarev [44] solved explicitly in 1877 in terms of elliptic functions. It is easy to see that up to a scalar scaling, the solution $R(x) \equiv x\frac{P(x^2)}{Q(x^2)}$ of (3.1) is identical to the solution of the min-max problem

$$\min_{R\in\mathcal{R}_{2r+1,2r}} \max_{x\in[-1,-\ell]\cup[\ell,1]} \left|\mathrm{sign}(x) - R(x)\right|. \tag{3.2}$$

For any $0 < \ell < 1$ and integer $r \geq 0$, problem (3.2) has a unique solution, which we donate by $Z_{2r+1}(x;\ell) \in \mathcal{R}_{2r+1,2r}$. We call $Z_{2r+1}(x;\ell)$ the *type* $(2r+1, 2r)$ *Zolotarev function*[2] corresponding to ℓ. As shown by Zolotarev [44] (see, e.g., [2, Ch. 9] or [3, Add. E]), the solution of (3.2) is given by

$$Z_{2r+1}(x;\ell) := Mx\prod_{j=1}^{r}\frac{x^2 + c_{2j}}{x^2 + c_{2j-1}}. \tag{3.3}$$

Here, the constant $M > 0$ is uniquely determined by the condition

$$1 - Z_{2r+1}(1;\ell) = -\big(1 - Z_{2r+1}(\ell;\ell)\big),$$

and the coefficients $c_1, c_2, \ldots, c_{2r}$ are given by

$$c_i = \ell^2\,\frac{\mathrm{sn}^2\left(\frac{iK'}{2r+1};\ell'\right)}{\mathrm{cn}^2\left(\frac{iK'}{2r+1};\ell'\right)}, \quad i = 1, 2, \ldots, 2r. \tag{3.4}$$

In (3.4),

$$l' = \sqrt{1-\ell^2}, \quad K' = \int_0^{\pi/2}\frac{d\theta}{\sqrt{1-(\ell')^2\sin^2\theta}}, \tag{3.5}$$

and $\mathrm{sn}(u;\ell')$ and $\mathrm{cn}(u;\ell')$ are the Jacobi elliptic functions (see, e.g., [1, Ch. 17] or [2, Ch. 5]). ℓ is called the modulus, ℓ' the complementary modulus, and K' the complete

[2]The index "$2r+1$", rather than "r", for the Zolotarev function Z_{2r+1} is used to facilitate the statement of the composition property of Zolotarev functions derived below.

elliptic integral of the first kind for the complementary modulus. For later use, we note that as shown in [3, Add. E], the maximum

$$\|\mathrm{sign}(\,\cdot\,) - Z_{2r+1}(\,\cdot\,;\ell)\|_\infty := \max_{x\in[-1,-\ell]\cup[\ell,1]} |\mathrm{sign}(x) - Z_{2r+1}(x;\ell)|$$

is attained at exactly $2r+2$ points $x_1 := \ell < x_2 < \cdots < x_{2r+1} < x_{2r+2} := 1$ in the interval $[\ell, 1]$ and also at exactly $2r+2$ points $x_{-j} := -x_j$, $j = 1, 2, \ldots, 2r+2$, in the interval $[-1, -\ell]$. Furthermore, the function $\mathrm{sign}(x) - Z_{2r+1}(x;\ell)$ equioscillates between the x_j's, in particular,

$$1 - Z_{2r+1}(x_j;\ell) = (-1)^{j+1}\,\|\mathrm{sign}(\,\cdot\,) - Z_{2r+1}(\,\cdot\,;\ell)\|_\infty\,, \quad j = 1, 2, \ldots, 2r+2. \tag{3.6}$$

3.1.1. Quality of $Z_{2r+1}(x;\ell)$ as approximants to $\mathrm{sign}(x)$**.** To illustrate the power of Zolotarev functions as approximants to $\mathrm{sign}(x)$, for $r = 1, 2, \ldots, 6$ and $\ell = 10^{-3}$, we plot $Z_{2r+1}(x;\ell)$ for $0 \le x \le 1$ in Figures 3.1(a)–(f); this suffices for an illustration as $Z_{2r+1}(x;\ell)$ is an odd function. Observe that as r increases, the Zolotarev function quickly becomes a very good approximation to the sign function.

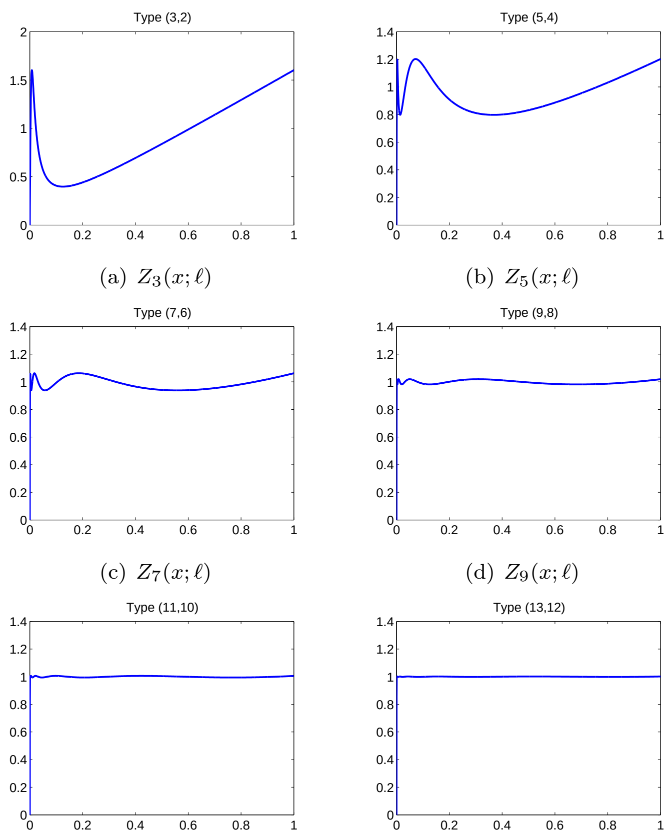

(a) $Z_3(x;\ell)$ (b) $Z_5(x;\ell)$

(c) $Z_7(x;\ell)$ (d) $Z_9(x;\ell)$

(e) $Z_{11}(x;\ell)$ (f) $Z_{13}(x;\ell)$

FIG. 3.1. *Zolotarev functions $Z_{2r+1}(x;\ell)$ of type $(2r+1, 2r)$ for $r = 1, 2, \ldots, 6$ and $\ell = 10^{-3}$*

The quality of Zolotarev functions as approximants to $\mathrm{sign}(x)$ is known to improve exponentially with the degree $n = 2r + 1$ [36, Sec. 4.3]:

$$\|\text{sign}(\,\cdot\,) - Z_n(\,\cdot\,;\ell)\|_\infty \approx C \exp\left(\frac{-cn}{\log(1/\ell)}\right) \tag{3.7}$$

for some constants $C, c > 0$. Furthermore, it is known that $C \approx 1$ [18, 29].

3.2. Rational function for Zolo-pd. For the following, it will be convenient to use the scaled Zolotarev function

$$\hat{Z}_{2r+1}(x;\ell) := \frac{Z_{2r+1}(x;\ell)}{Z_{2r+1}(1;\ell)}.$$

We remark that $\hat{Z}_{2r+1}(x;\ell)$ maps the set $[-1,-\ell] \cup [\ell, 1]$ onto $[-1, -\tilde{\ell}] \cup [\tilde{\ell}, 1]$, where $\tilde{\ell} := \min_{x\in[\ell,1]} \hat{Z}_{2r+1}(x;\ell) = \hat{Z}_{2r+1}(\ell;\ell)$. Note that, using (3.6), one can easily verify that $0 < \tilde{\ell} < 1$.

Combining the iterative process used in QDWH and the scaled Zolotarev functions just described, we arrive at an algorithm that approximates the sign function by composing Zolotarev functions: Starting with an interval $[\ell, 1]$ with $0 < \ell < 1$ that contains all the singular values of A, we set $\ell_0 := \ell$ and form $R_1 := \hat{Z}_{2r+1}(x;\ell_0)$, the scaled r-th Zolotarev function corresponding to ℓ_0, which maps $[-1,-\ell_0] \cup [\ell_0, 1]$ onto $[-1,-\ell_1] \cup [\ell_1, 1]$. Here, $\ell_1 := R_1(\ell_0)$ with $\ell_1 > \ell_0$, typically $|1-\ell_1| \ll |1-\ell_0|$. Then we form the r-th scaled Zolotarev function $R_2 := \hat{Z}_{2r+1}(x;\ell_1)$ corresponding to ℓ_1, which maps $[-1,-\ell_1] \cup [\ell_1, 1]$ onto $[-1,-\ell_2] \cup [\ell_2, 1]$, where $\ell_2 := R_2(\ell_1)$ and $\ell_2 > \ell_1$. The composed function $R_2(R_1(x))$ maps the original set $[-1,-\ell] \cup [\ell, 1]$ onto $[-1,-\ell_2] \cup [\ell_2, 1]$. Repeating this process k times we obtain $[\ell_k, 1] = R_k([\ell_{k-1}, 1])$ with $|1-\ell_k| \ll |1-\ell_{k-1}|$; our algorithm Zolo-pd actually needs only $k = 2$ iterations.

3.3. Composed Zolotarev functions are again Zolotarev functions. The algorithm just described employs a composed rational function $R(x) := \hat{Z}_{2r+1}\big(\hat{Z}_{2r+1}(x;\ell);\ell_1\big)$ that approximates the sign function on the interval $[-1,-\ell]\cup[\ell,1]$, in which both components are scaled Zolotarev functions, but corresponding to the different values ℓ and ℓ_1. The composed function R is clearly a rational function in $\mathcal{R}_{(2r+1)^2,(2r+1)^2-1}$, and thus we have 'squared' the degree of $\hat{Z}_{2r+1}(x;\ell)$.

In this subsection, we show that $R(x) = \hat{Z}_{(2r+1)^2}(x;\ell)$, i.e, R is indeed the scaled Zolotarev function of squared type $((2r+1)^2, (2r+1)^2-1)$ corresponding to the original value of ℓ. Similarly, we can compose k Zolotarev functions to obtain $R_k(\cdots R_2(R_1(x))\cdots) = \hat{Z}_{(2r+1)^k}(x;\ell)$ where each $R_i \in \mathcal{R}_{2r+1,2r}$ is the scaled Zolotarev function of type $(2r+1, 2r)$ corresponding to ℓ_{i-1}, where $\ell_i := \min_{x\in[\ell_{i-1},1]} \hat{Z}_{2r+1}(x;\ell_{i-1}) = \hat{Z}_{2r+1}(\ell_{i-1};\ell_{i-1})$.

We emphasize that the fact that a high-degree best rational approximant is obtained as the composition of low-degree rational approximants is a remarkable special property enjoyed by the sign function, since k odd rational functions $R_1, \ldots, R_k \in \mathcal{R}_{2r+1,2r}$ altogether have only $k(2r+1)$ parameters, whereas general rational functions in $\mathcal{R}_{(2r+1)^k,(2r+1)^k-1}$ have $2(2r+1)^k$ degrees of freedom.

3.3.1. Best rational approximation on union of two intervals. To prove this fact, we need a classical result on the characterization of best rational approximants called *equioscillation* [36, 37, 39]. Consider the problem of approximating a given continuous function $F : [a, b] \mapsto \mathbb{R}$ on a real interval $[a, b]$ by a rational function $R \in \mathcal{R}_{m,n}$ (in this subsection only, m, n denote the degrees, not the matrix size):

$$\min_{R\in\mathcal{R}_{m,n}} \|F-R\|_\infty\,, \quad \text{where} \quad \|F-R\|_\infty := \max_{x\in[a,b]} |F(x)-R(x)|\,.$$

We say that the error $F - R$ *equioscillates* between k *extreme points* if there exist $a \leq x_1 < x_2 < \cdots < x_k \leq b$ such that

$$F(x_j) - R(x_j) = \rho(-1)^j \|F - R\|_\infty \quad j = 1, 2, \ldots, k, \tag{3.8}$$

where ρ is either 1 or -1. The *defect* of a rational function $R = \frac{P}{Q} \in \mathcal{R}_{m,n}$ in $\mathcal{R}_{m,n}$ is defined as $d(R) := \min\{m - \deg P, n - \deg Q\}$ if $R \not\equiv 0$ and $d(R) = 0$ if $R \equiv 0$. The classical characterization of best rational approximant can be stated as follows.

Lemma 3.1. *Let $F : [a,b] \mapsto \mathbb{R}$ be a continuous function. Then, $R \in \mathcal{R}_{m,n}$ is the unique best rational approximant of F in $\mathcal{R}_{m,n}$ if, and only if, $F - R$ equioscillates between at least $m+n+2-d(R)$ extreme points, where d is the defect of R in $\mathcal{R}_{m,n}$.*

In what follows, all the rational functions we consider have maximum possible numerator and denominator degree in $\mathcal{R}_{m,n}$ so that the defect $d = 0$. Regardless of d, Lemma 3.1 shows that equioscillation of $F - R$ at $m + n + 2$ extreme points is a sufficient condition for optimality. For our specific problem of approximating the sign function, we work with a union of two intervals $[-1, -\ell] \cup [\ell, 1]$, and in particular we use the following sufficient condition for optimality (see also [36, Thm 4.4]). For a union $[a, c] \cup [d, b]$, where $a < c < d < b$, we still say $F - R$ equioscillates between k extreme points if (3.8) holds for k distinct increasing points $x_j \in [a, c] \cup [d, b]$.

Lemma 3.2. *Let $F : [a,c] \cup [d,b] \mapsto \mathbb{R}$ be a continuous function and $a < c < d < b$. Then, $R \in \mathcal{R}_{m,n}$ is the unique best rational approximant of F in $\mathcal{R}_{m,n}$ if $F - R$ equioscillates between at least $m + n + 3$ extreme points.*

Note that the number of extreme points $m+n+3$ is one larger than in Lemma 3.1 for the case of a single interval $[a, b]$, and the lemma gives a sufficient condition for optimality, which may not be a necessary condition.

Proof. Suppose $F - R$ equioscillates between $m + n + 3$ extreme points satisfying (3.8) for $\{x_j\}_{j=1}^{m+n+3}$, and suppose there exists a better approximation $\tilde{R} \in \mathcal{R}_{m,n}$ such that $\|F - \tilde{R}\|_\infty < \|F - R\|_\infty$. Then $R - \tilde{R}$ must take alternating signs at the points x_j, which means it must be 0 in at least $m + n + 3 - 2 = m + n + 1$ distinct points[3], each in $[x_j, x_{j+1}]$, possibly except for the one that contains $\frac{c+d}{2}$. However, since $R - \tilde{R} \in \mathcal{R}_{m+n,2n}$, it cannot have more than $m + n$ zeros unless $R - \tilde{R} = 0$. □

Applying Lemma 3.2 to the case $F = \mathrm{sign}(x)$ on $[-1, -\ell] \cup [\ell, 1]$ shows that given a rational function $R \in \mathcal{R}_{2r+1,2r}$, we can test its optimality by counting the number of equioscillation points and by checking if this number is at least $2r+1+2r+3 = 4r+4$. For example, in view of (3.6), Zolotarev functions $Z_{2r+1}(x; \ell) \in \mathcal{R}_{2r+1,2r}$ satisfy this property. Observe that each Zolotarev function in Figures 3.1(a)-3.1(f) has exactly $2r+2$ equioscillation points in $[\ell, 1]$ (the fact that F is the sign function makes counting the equioscillation points straightforward), and by the symmetry about the origin, in total there are $4r+4$ equioscillation points, verifying its optimality as the best rational approximant.

3.3.2. Equioscillation of composed Zolotarev functions. We now show that the composed scaled Zolotarev function $\hat{Z}_{2r+1}\big(\hat{Z}_{2r+1}(x; \ell); \ell_1\big)$ is indeed a scaled Zolotarev function of higher type.

Theorem 3.3. *Let $\hat{Z}_{2r+1}(x; \ell) \in \mathcal{R}_{2r+1,2r}$ be the scaled Zolotarev function corresponding to $\ell \in (0, 1]$, and let $\hat{Z}_{2r+1}(x; \ell_1) \in \mathcal{R}_{2r+1,2r}$ be the scaled Zolotarev function corresponding to $\ell_1 := \hat{Z}_{2r+1}(\ell; \ell)$. Then*

$$\hat{Z}_{2r+1}\big(\hat{Z}_{2r+1}(x; \ell); \ell_1\big) = \hat{Z}_{(2r+1)^2}(x; \ell). \tag{3.9}$$

[3]This number would be $m + n + 2$ if we have only a single interval instead of a union of two intervals.

Moreover, defining ℓ_i iteratively by $\ell_{i+1} := \hat{Z}_{2r+1}(\ell_i;\ell_i)$, after k iterations we have

$$\hat{Z}_{2r+1}(\cdots\hat{Z}_{2r+1}(\hat{Z}_{2r+1}(x;\ell);\ell_1);\cdots;\ell_{k-1}) = \hat{Z}_{(2r+1)^k}(x;\ell), \tag{3.10}$$

the scaled Zolotarev function of type $((2r+1)^k,(2r+1)^k-1)$.

Proof. We first prove (3.9). The function $\hat{Z}_{2r+1}\big(\hat{Z}_{2r+1}(x;\ell);\ell_1\big)$ is clearly a rational function of type $((2r+1)^2,(2r+1)^2-1)$. Thus, by Lemma 3.2, it suffices to prove that $\tilde{M}_2\operatorname{sign}(x) - \hat{Z}_{2r+1}(\hat{Z}_{2r+1}(x;\ell);\ell_1)$ equioscillates between at least $(2r+1)^2+(2r+1)^2-1+3 = 2(2r+1)^2+2$ extreme points in $[-1,-\ell]\cup[\ell,1]$ for some $\tilde{M}_2>0$ (indeed $\tilde{M}_2=(\ell_2+1)/2$; in general we define $\tilde{M}_i=(\ell_i+1)/2$ for $i\in\mathbb{N}$). By symmetry it suffices to show that $\tilde{M}_2-\hat{Z}_{2r+1}(\hat{Z}_{2r+1}(x;\ell);\ell_1)$ equioscillates between at least $(2r+1)^2+1$ extreme points in the positive interval $[\ell,1]$.

In view of (3.6), the function $\tilde{M}_1-\hat{Z}_{2r+1}(x;\ell)$ equioscillates between the $2r+2$ points $(\ell=)x_1<x_2<\cdots<x_{2r+2}(=1)$. Consider the intervals $[x_j,x_{j+1}]$ for $j=1,\ldots,2r+1$. The function $\hat{Z}_{2r+1}(x;\ell)$ is continuous and maps each $[x_j,x_{j+1}]$ onto the interval $[\ell_1,1]$, which is then mapped by $\hat{Z}_{2r+1}(x;\ell_1)$, in such a way that $\tilde{M}_2-\hat{Z}_{2r+1}\big(\hat{Z}_{2r+1}(x;\ell);\ell_1\big)$ has $2r+2$ equioscillation points on $[x_j,x_{j+1}]$, including those precisely at x_j,x_{j+1}. Hence summing up the equioscillation points on $[\ell,1]$ gives $(2r+1)(2r+2)-2r$ points, in which the subtraction of $2r$ accounts for the double-counted points x_i for $j=2,\ldots,2r+1$. Since $(2r+1)(2r+2)-2r=(2r+1)^2+1$, we thus have the required number of equioscillation points.

The proof for the general statement (3.10) is essentially the same by induction: after $k-1$ iterations we have $\hat{Z}_{(2r+1)^{k-1}}(x;\ell)$, which has the property that $\tilde{M}_{k-1}-\hat{Z}_{(2r+1)^{k-1}}(x;\ell)$ equioscillates between the $(2r+1)^{k-1}+1$ points $(\ell_{k-1}=)x_1<\cdots<x_{(2r+1)^{k-1}+1}(=1)$. Each interval $[x_j,x_{j+1}]$ for $j=1,\ldots,(2r+1)^{k-1}$ is mapped by $\hat{Z}_{(2r+1)^{k-1}}(x;\ell)$ to $[\ell_k,1]$, which is then mapped by $\hat{Z}_{2r+1}(x;\ell_{k-1})$, in such a way that $\tilde{M}_k-\hat{Z}_{2r+1}\big(\hat{Z}_{(2r+1)^{k-1}}(x;\ell);\ell_{k-1}\big)$ has $2r+2$ equioscillation points on $[x_j,x_{j+1}]$, including x_j,x_{j+1}. Hence summing up the equioscillation points on $[\ell,1]$ gives $(2r+1)^{k-1}(2r+2)-2(2r+1)^{k-1}=(2r+1)^k+1$ points, completing the proof. □

Figure 3.2 gives an illustration for $r=1$, $k=2$ and $\ell=\frac{1}{500}$. The red points are the equioscillation points x_j of $\tilde{M}_1-\hat{Z}_{2r+1}(x;\ell)$, with each $[x_j,x_{j+1}]$ being mapped to $[\ell_1,1]$ with $\ell_1\approx 0.31$. The black points are equioscillation points of $\tilde{M}_2-\hat{Z}_{2r+1}(x;\ell_1)$, which generate equioscillation points at the x-values of the blue points. Shown in dashed pink is the composed Zolotarev function $\hat{Z}_{2r+1}(\hat{Z}_{2r+1}(x;\ell);\ell_1)=\hat{Z}_{(2r+1)^2}(x;\ell)$.

3.4. Benefits of computing $\hat{Z}_{(2r+1)^k}(x,\ell)$ by composition. There are two ways to compute $\hat{Z}_{(2r+1)^k}(x;\ell)$, eventually at a matrix argument $x=A$.

1. Directly by (3.3).
2. Compute k Zolotarev functions $\hat{Z}_{2r+1}(x;\ell),\hat{Z}_{2r+1}(x;\ell_1),\ldots,\hat{Z}_{2r+1}(x;\ell_{k-1})$ and then form $\hat{Z}_{2r+1}(\cdots\hat{Z}_{2r+1}(\hat{Z}_{2r+1}(x;\ell);\ell_1)\cdots);\ell_{k-1})$.

We argue that the second approach by composition is significantly better, both in speed and numerical stability.

Regarding the speed, let us compare the evaluations $Z=\hat{Z}_{(2r+1)^k}(A;\ell)$ and $\hat{Z}_{2r+1}(\cdots(\hat{Z}_{2r+1}(A;\ell);\cdots);\ell_{k-1})$ at a matrix A. Using the partial fraction representation (discussed in Section 4.1) the direct evaluation of $\hat{Z}_{(2r+1)^k}(A;\ell)$ requires $\frac{(2r+1)^k-1}{2}$ matrix operations (QR factorizations and matrix multiplications). By contrast, consider computing $\hat{Z}_{2r+1}(\cdots(\hat{Z}_{2r+1}(A;\ell);\cdots);\ell_{k-1})$, which we do sequentially

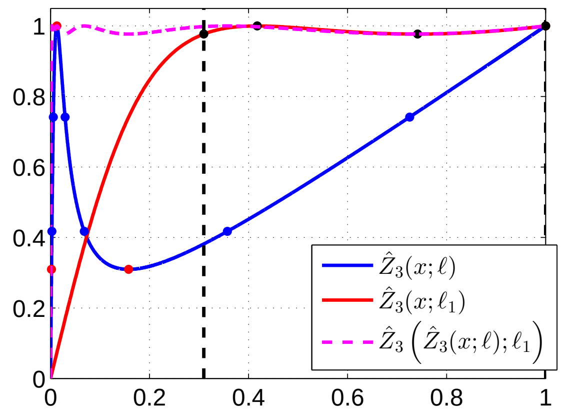

FIG. 3.2. *Zolotarev functions $\hat{Z}_3(x;\ell)$ (blue), $\hat{Z}_3(x;\ell_1)$ (red) and its composition (pink) $\hat{Z}_3\left(\hat{Z}_3(x;\ell);\ell_1\right) = \hat{Z}_9(x;\ell)$ for $\ell = \frac{1}{500}$, and their equioscillation points.*

as follows: $B_1 = \hat{Z}_{2r+1}(A;\ell)$, $B_{i+1} = \hat{Z}_{2r+1}(B_i;\ell_i)$ for $i = 1,\dots,k-1$, and $Z = B_{k-1}$. Since forming B_i needs just one matrix operation for each i, this evaluation uses rk matrix operations. Clearly $\frac{(2r+1)^k-1}{2} \gg rk$ for $k > 1$ with difference growing exponentially with k, so evaluation by composition is much more efficient. Essentially the same argument holds when the input A is a scalar.

Concerning stability, Figure 3.3 shows the error $\left\|\text{sign}(\,\cdot\,) - Z_{(2r+1)^2}(\,\cdot\,;\ell)\right\|_\infty$ of the computed Zolotarev functions. We take various values of $\ell := 1/\kappa$, in which κ represents the matrix condition number in Zolo-pd, since $[\ell, 1]$ contains the singular values of $X_0 = A/\alpha$: recall that $\ell = 1/\kappa_2(A)$ when exact estimates $\alpha = \|A\|_2$ and $\ell = \sigma_{\min}(X_0)$ are used. The blue plots are from direct computation. Composition-based computation takes isolated values: the red circles show $r = 1$, so they take degrees $(3^k, 3^k - 1)$, and the black triangles are $r = 7$. The red dashed lines illustrate the theoretical asymptotic convergence.

Observe that the blue plots stagnate at some threshold, showing that computing high-degree Zolotarev functions directly is unstable for high degree (this is with the "robust" way of computing the elliptic functions as discussed in Section 4.3). Indeed, some of the coefficients c_{2j-1}, c_{2j} in (3.3) become very small as r grows, and relative precision is lost when dealing with terms like $x^2 + c_{2j-1}$, even if c_{2j-1} was computed very accurately. By contrast, computation by composition is accurate even when the degree $(2r + 1)^k$ is high. This is because each low-degree Zolotarev function $\hat{Z}_{2r+1}(A;\ell_i)$ is computed accurately, and hence so is its composition.

3.5. Choice of the integer r. Choosing a larger value of r increases the degree of the Zolotarev functions in $\mathcal{R}_{2r+1,2r}$, leading to an improved approximation to $\text{sign}(x)$ as predicted by (3.7) and illustrated in Figure 3.1. This means the iteration generally converges in fewer steps by taking r larger. However, the arithmetic cost per iteration grows with r, and taking r too large can lead to numerical instability as we just saw.

The key to the optimal choice of r is to have an accurate estimate of the number of iterations required for convergence. Specifically, recalling Section 2.1 and the fact that k iterations of Zolo-pd employs $\hat{Z}_{(2r+1)^k}(x;\ell)$, the number of iterations required

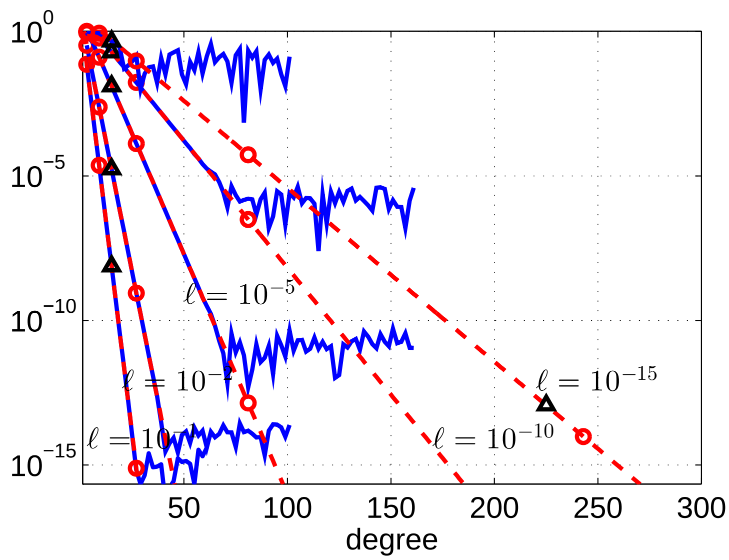

FIG. 3.3. *Zolotarev functions computed directly (blue) and via composition (red circle for $r = 1$, blue triangles for $r = 7$). The horizontal axis is the degree of the numerator polynomial of the Zolotarev function.*

is essentially the smallest value of k for which $\hat{Z}_{(2r+1)^k}([\ell, 1]; \ell) \subseteq [1 - \mathcal{O}(u), 1]$. This argument is much in the same vein as those in the literature for the scaled Newton iteration [20, p. 206] and the QDWH iteration [31]. Table 3.1 shows the smallest k for which $\hat{Z}_{(2r+1)^k}([\frac{1}{\kappa_2(A)}, 1]; \ell) \subseteq [1 - 10^{-15}, 1]$ for varying values of r and $\ell = \frac{1}{\kappa_2(A)}$. Observe that the Zolotarev approximants with moderately large r are so powerful that *two* iterations is enough for convergence for a wide range of $\kappa_2(A)$.

TABLE 3.1
Required number of iterations for varying $\kappa_2(A)$ and r, obtained as the smallest k for which $\hat{Z}_{(2r+1)^k}([\ell, 1])) \subseteq [1 - \mathcal{O}(u), 1]$.

$\kappa_2(A)$	1.001	1.01	1.1	1.2	1.5	2	10	10^2	10^3	10^5	10^7	10^{16}
$r = 1$ (QDWH)	2	2	2	3	3	3	4	4	4	5	5	6
$r = 2$	1	2	2	2	2	2	3	3	3	3	4	4
$r = 3$	1	1	2	2	2	2	2	2	3	3	3	3
$r = 4$	1	1	1	2	2	2	2	2	2	3	3	3
$r = 5$	1	1	1	1	2	2	2	2	2	2	3	3
$r = 6$	1	1	1	1	1	2	2	2	2	2	2	3
$r = 7$	1	1	1	1	1	1	2	2	2	2	2	3
$r = 8$	1	1	1	1	1	1	2	2	2	2	2	2

In light of this, in Figure 3.4 we show the value of r required for the iteration to converge in two steps for varying condition numbers $\kappa_2(A) = \frac{1}{\ell}$. For matrices of practical interest $\kappa_2(A) \geq u^{-1}$, we need a Zolotarev function of type about $(281, 280)$ or higher for numerical convergence. Since two iterations with $r = 8$ gives a type $(289, 288)$ Zolotarev function, it follows that we can take $r \leq 8$ in double precision arithmetic to obtain an algorithm that converges in two steps.

When $\kappa_2(A)$ happens to be well conditioned so that $\kappa_2(A) \leq 2$, one iteration is enough by taking r to be the value for which the entry is 1 in Table 3.1 (with

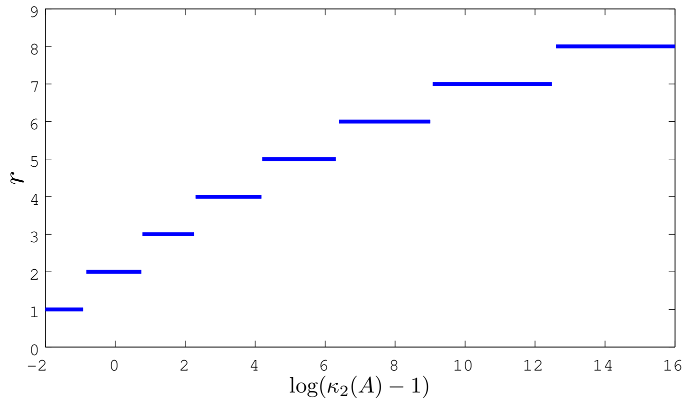

FIG. 3.4. *Degree of polynomials r needed for convergence in two iterations.*

a Cholesky-based efficient implementation; see Section 5.1). In the context of the symmetric eigendecomposition, our primary interest is in $\kappa_2(A) \simeq n$ because this is the average-case scenario of the condition number of a shifted matrix $A := A - \sigma I$ where σ is a scalar parameter that we can choose. For practical values $\kappa_2(A) \leq 10^5$, $r \leq 5$ is enough to obtain convergence in two iterations.

3.6. Convergence rate. Although our algorithm converges in two steps, it is still an iterative method; after all, the polar decomposition is not finitely computable [13]. Therefore a valid question arises: what is the convergence rate? The answer is $2r+1$, which can be as high as 17, as we take r to be up to 8.

Verifying this is straightforward. We denote the error after k iterations of composing Zolotarev functions of type $(2r+1, 2r)$ by

$$\text{error}_k := \max_{x \in [-1,-\ell] \cup [\ell,1]} |\operatorname{sign}(x) - Z_{(2r+1)^k}(x;\ell)|, \tag{3.11}$$

which is the error of the approximant employed by k iterations of Zolo-pd.

THEOREM 3.4. *Let r be an integer and $\ell \in (0,1)$. Then the error after k iterations as in* (3.11) *converges to* 0 *with convergence rate* $2r+1$*, that is,*

$$\text{error}_{k+1} = C_r \big(\text{error}_k\big)^{2r+1} \tag{3.12}$$

for some constant C_r.

Proof. Recall that the error of the Zolotarev functions decays exponentially with the degree as in (3.7), which recalling $\kappa = 1/\ell$ we write $C \exp\left(\frac{-cn}{\log \kappa}\right)$. Hence the error after $k+1$ iterations is

$$\begin{aligned} \text{error}_{k+1} &= \max_{x \in [-1,-\ell] \cup [\ell,1]} |Z_{(2r+1)^{k+1}}(x;\ell) - \operatorname{sign}(x)| \\ &\approx C \exp\left(\frac{-c(2r+1)^{k+1}}{\log \kappa}\right) \\ &= C\left(\exp\left(\frac{-c(2r+1)^k}{\log \kappa}\right)\right)^{2r+1} \approx C_r \big(\text{error}_k\big)^{2r+1} \end{aligned} \tag{3.13}$$

where $C_r = C^{-2r}$, completing the proof. ∎

The order $2r+1=17$ convergence in Zolo-pd $\text{error}_{k+1} = \mathcal{O}(\text{error}_{k+1})^{17}$ is deceptively fast: once we have $\text{error}_k \lesssim 0.1$, one more iteration is enough to give convergence to machine precision. Indeed this is a reasonably accurate illustration of what the algorithm does, as the first iteration maps the interval $[-1,-\ell]\cup[\ell,1]$ to $[-1,-\ell_1]\cup[\ell_1,1]$ with $1-\ell_1$ is $\mathcal{O}(0.1)$, and the second iteration maps $[-1,-\ell_1]\cup[\ell_1,1]$ to $[-1,-\ell_2]\cup[\ell_2,1]$ with $|\ell_2-1|\approx|\ell_1-1|^{17}\lesssim u$.

Of course, there is nothing sacred about the specific number 17; it just happens to be the smallest value of $2r+1$ for which the error after two iterations is $\mathcal{O}(u)$ for $\ell=u$ in double precision arithmetic $u\approx 10^{-16}$. For example, in quadruple precision in which $u\approx 10^{-32}$ we will need $r=16$ with convergence rate 33 for a two-step convergent algorithm, and in single precision $u\approx 10^{-8}$ it suffices to take $r=4$.

3.7. Related studies on Zolotarev functions. Zolotarev's functions have a long and rich history. Regarding the result "composed Zolotarev is high-degree Zolotarev", a related observation has been made by Ninomiya [34] and Braess [9] for the square root function, in the context of accelerating Herron's iteration. They observe that by appropriately scaling Herron's iteration, which composes type $(2,1)$ approximants in each iteration, one can obtain the best rational approximant to the square root function, in terms of minimizing the relative error $\|\frac{\frac{p(\,\cdot\,)}{q(\,\cdot\,)}-\sqrt{\cdot}}{\sqrt{\cdot}}\|_\infty$. Recently Beckerman [8] revisited this observation in the context of the matrix square root.

The best rational approximants for the square root on $[\ell,1]$ and that for the sign function Z_{2r+1} are related by the fact that $Z_{2r+1}(x;\ell)=x\frac{P_r(x^2)}{Q_r(x^2)}\approx \text{sign}(x)$ implies $\frac{P_r(x)}{Q_r(x)}\approx\sqrt{x}$ for $[\ell,1]$, and vice versa. Hence by using the results of Ninomiya and Braess one can obtain Theorem 3.3 for composing Zolotarev functions of type $(2,1)$. This work extends the observation to composing rational approximants of arbitrary degrees, and revisits the connection between the best rational approximants for the sign and square root functions.

Van den Eshof and his coauthors [40, Sec. 4.5.2],[41] used Zolotarev's results to approximate $\text{sign}(A)x$ for a given vector x and symmetric A (note that $U_p=\text{sign}(A)$ for symmetric A). To compute $\text{sign}(A)x$ efficiently, they find the lowest degrees of P and Q such that the computed result has acceptable error (which they set to $\approx 10^{-2}$). A recent work of Güttel, Polizzi, Tang and Viaud [18] computes partial eigenpairs of large-sparse matrices using Zolotarev functions: they apply $Z_{2r+1}(A;\ell)$ to a vector (or a set of vectors) to obtain a "filter function" that gives a subspace rich in the eigenspace corresponding to the eigenvalues of A in a specified interval, and repeatedly apply the filter function to improve the accuracy. Druskin, Güttel, and Knizhnerman [12] use Zolotarev's function for the inverse square root function. The crucial difference from these studies is that we employ a matrix iteration and compute the entire unitary polar factor U_p, instead of its action on a vector. This permits us to iterate on the computed result, and thus to form composed rational functions. The difference is exponential: applying the filter function repeatedly k times gives error $C\exp(\frac{-ckn}{\log\ell})$, whereas composing k times gives $C\exp(\frac{-cn^k}{\log\ell})$.

As a consequence, the accuracy to working precision in double precision arithmetic is achievable without involving a very high-degree rational function (we need $r=8$ or smaller, as opposed to $r\geq 140$ to get a single-step convergence to the tolerance u).

While some studies use the type $(2r-1,2r)$ Zolotarev functions, we focus on type $(2r+1,2r)$ functions because this results in a slightly better approximation since $\mathcal{R}_{2r-1,2r}\in\mathcal{R}_{2r+1,2r}$, and they require the same computational cost to evaluate at a matrix argument.

In the conclusion of [23] Iannazzo compares the iteration via Padé approximant with the best rational approximant and notes that while Padé gives an order of convergence larger than 1, it requires degree much higher than the best rational approximant, so it is unclear which is more efficient. This work gives a clear answer for the sign function, which gets the best of both worlds: we obtain the highest possible order of convergence while simultaneously using the best rational approximant. Other cases in which Zolotarev's rational approximation is used in the context of matrix iterations include [19, 25, 27].

One may have wondered why we have restricted ourselves to odd rational functions, when the goal is to map the singular values, which are nonnegative numbers, to 1: perhaps a non-odd function that focuses on $[\ell, 1]$ would be more effective. However, a matrix expressed as $Uf(\Sigma)V^*$ is generally difficult to compute unless $f(\Sigma)$ is an odd function; for example computing $U\Sigma^2V^*$ without the knowledge of the polar decomposition or SVD is already nontrivial. If f is odd so that $f(x) = x\frac{P(x^2)}{Q(x^2)}$ then we can compute $Uf(\Sigma)V^* = AP(A^*A)Q(A^*A)^{-1}$; we will use its partial fraction form for its evaluation (see Section 4.1). Another explanation is that for the symmetric eigendecomposition, the goal of computing the polar decomposition of a shifted symmetric matrix $A - \sigma I$ is to split the spectrum into two distinct groups, so we need to map both (positive and negative) sides of the spectrum to distinct values, a natural choice of which is ± 1.

4. Implementation issues.

We now discuss the implementation of Zolo-pd for computing the polar decomposition of a matrix $A \in \mathbb{C}^{m\times n}$.

4.1. Evaluating $\hat{Z}_{2r+1}(x;\ell)$ at matrix arguments $\hat{Z}_{2r+1}(A;\ell)$.

To apply the Zolotarev functions to the singular values of A, we need an efficient and stable way of computing $R(X_k) = U\hat{Z}_{2r+1}(\Sigma_k;\ell)V^*$, where $X_k = U\Sigma_k V^*$ is the SVD. For stability and communication efficiency, we look for an inverse-free implementation, that is, one that does not explicitly invert matrices or require solutions to linear systems; this was the original motivation for the QDWH iteration [31].

Crucial to this task is the following result, which was given in [43], [20, p. 219], and was also used in the QDWH iteration (which is Zolo-pd for the special case $r = 1$).

LEMMA 4.1. *Let* $\begin{bmatrix}\eta X\\ I\end{bmatrix} = \begin{bmatrix}Q_1\\ Q_2\end{bmatrix} R$ *be the QR decomposition of* $\begin{bmatrix}\eta X\\ I\end{bmatrix}$*, where* $X, Q_1 \in \mathbb{C}^{m\times n}$ *and* $Q_2, R \in \mathbb{C}^{n\times n}$*. Then*

$$Q_1 Q_2^* = \eta X(I + \eta^2 X^* X)^{-1}. \tag{4.1}$$

We now show that by using the partial fraction representation of $Z_{2r+1}(x;\ell)$ we can use this lemma for the stable computation of $R(X)$ for any $r \geq 1$.

In general, a partial fraction representation expresses a given rational function in terms of a sum of fractions involving polynomials of low degree. For the Zolotarev function $\hat{Z}_{2r+1}(x;\ell)$ given by (3.3), we obtain the following partial fraction decomposition representation:

$$\hat{Z}_{2r+1}(x;\ell) = \prod_{j=1}^{r} \frac{x^2 + c_{2j}}{x^2 + c_{2j-1}} = 1 - \sum_{j=1}^{r} \frac{a_j}{x^2 + c_{2j-1}}, \tag{4.2}$$

where

$$a_j = \left(\prod_{k=1}^{r}(c_{2j-1} - c_{2k})\right) \cdot \left(\prod_{k=1, k\neq j}^{r}(c_{2j-1} - c_{2k-1})\right). \tag{4.3}$$

Equation (4.3) provides a simple and stable way to compute the coefficients a_j in (4.2), and an easy way to verify (4.3) is to multiply (4.2) by $x^2 + c_{2j-1}$ and take $x = ic_{2j-1}$.

In matrix form, our task is to compute

$$R(X) = X \prod_{j=1}^{r} P_j(X^*X) \prod_{j=1}^{r} (Q_j(X^*X))^{-1},$$

where $P_j(X^*X) = X^*X + c_{2j}I$ and $Q_j(X^*X) = X^*X + c_{2j-1}I$. Using (4.2), we see that $R(X)$ can be obtained by computing

$$R(X) = X + \sum_{j=1}^{r} a_j X(X^*X + c_{2j-1}I)^{-1}, \tag{4.4}$$

which, by Lemma 4.1, is equivalent to

$$\begin{cases} \begin{bmatrix} X \\ \sqrt{c_{2j-1}}I \end{bmatrix} = \begin{bmatrix} Q_{j1} \\ Q_{j2} \end{bmatrix} R_j, \\ R(X) = X + \sum_{j=1}^{r} \frac{a_j}{\sqrt{c_{2j-1}}} Q_{j1}Q_{j2}^*. \end{cases} \tag{4.5}$$

Note that the r QR factorizations and matrix multiplications $Q_{j1}Q_{j2}^*$ in (4.5) are completely independent of each other, therefore we can easily compute $Q_{j1}Q_{j2}^*$ in a parallel fashion for $j = 1, \ldots, r$ and compute $R(X)$ simply by adding up the matrices. Furthermore, numerically the evaluation (4.5) based on partial fractions is much more accurate than a direct evaluation.

We note that the use of partial fraction for Padé-type matrix iterations was employed by Kenney and Laub in [26] for the matrix sign function, and by Higham and Papadimitriou [21] for the polar decomposition. For the action of a matrix function on a vector it was used for example in [12, 41].

Single-iteration algorithm?. Due the the "embarrassing" parallelizability, increasing r further does not pose a serious computational bottleneck in a parallel implementation. Hence a natural idea is to choose r large enough so that a single iteration is enough to obtain the unitary polar factor, that is, $\hat{Z}_{2r+1}([1/\kappa_2(A), 1]; \ell) \subseteq [1 - \mathcal{O}(u), 1]$. However, the value r needed to achieve this grows rapidly with $\kappa_2(A) = 1/\ell$. The exponential decay of the error (3.7) with the degree means this number grows like $\mathcal{O}(\log \kappa_2(A))$, and it is about $\frac{280}{2}$ when $\kappa_2(A) \approx 10^{16}$. Besides the obvious increase in the arithmetic cost, taking r this large entails the serious numerical instability observed in Figure 3.3.

In Zolo-pd, by allowing for the second iteration we reduce r from $\mathcal{O}(\log \kappa_2(A))$ to $\mathcal{O}(\sqrt{\log \kappa_2(A)})$. This improves the stability dramatically as we saw in Figure 3.3. Moreover, the overhead in speed of allowing the second iteration is marginal, and in fact the runtime is much less than doubled. This is because the second iteration can be executed more efficiently than the first using the Cholesky factorization, as we discuss next.

4.2. Using the Cholesky factorization in the second iteration. Recall that the iterate (4.5) is mathematically equivalent to (4.4), which can be computed (more directly) via

$$\begin{cases} Z_{2j-1} = X^*X + c_{2j-1}I, \quad W_{2j-1} = \mathrm{Chol}(Z_{2j-1}), \\ R(X) = X + \sum_{j=1}^{r} a_j (XW_{2j-1}^{-1})W_{2j-1}^{-*}. \end{cases} \tag{4.6}$$

When X is well-conditioned, it is preferable to execute (4.6) instead of (4.5) for efficiency as discussed in [33] in the context of QDWH. The arithmetic cost of (4.6) is $3mn^2 + n^3/3$ and that of (4.5) is $5mn^2$ for each j.

Since the error bound in performing the Cholesky factorization $W_{2j-1} = \mathrm{Chol}(Z_{2j-1})$ is proportional to the condition number $\kappa_2(Z_{2j-1}) = \kappa_2(X^*X + c_{2j-1}I)$, in [33] the iteration switches to the Cholesky-based implementation when $\kappa_2(Z_{2j-1}) \le 100$ is guaranteed, for which $\kappa_2(X) \le 10$ is a sufficient condition.

Fortunately, in practice we always have $\kappa_2(Z_{2j-1}) \le 3$ for the second iteration in Zolo-pd. This is because the type $(2r+1, 2r)$ rational approximation to $\mathrm{sign}(x)$ on $[-1, -\ell] \cup [\ell, 1]$ with $\ell = 10^{15}$ and $r = 8$ maps the singular values to $\hat{Z}_{17}([10^{-15}, 1]; 10^{-15}) \subseteq [.39, 1]$. This can be seen also from Table 3.1, which shows that we need $\kappa_2(A) \lesssim 2$ to get convergence in one step with $r \le 8$; more precisely we need $\kappa_2(A) \lesssim 2.6$. Since the interval $[10^{-15}, 1]$ is mapped to $[1-u, 1]$ in two iterations, one iteration must result in an interval contained in $[\frac{1}{2.6}, 1] \supseteq [.39, 1]$.

Hence the second iteration can be safely computed via (4.6) using the Cholesky factorization. In fact, experiments suggest that using (4.6) for the second iteration improves not only the speed but also slightly the stability. To summarize, the first iteration of Zolo-pd needs to be executed as in (4.5), and it is recommended that the second iteration be computed by (4.6).

We note that for well-conditioned A we can make Zolo-pd more efficient. Specifically, if $\kappa_2(A)$ (or its estimate) is smaller than 2, then we find from Table 3.1 the smallest r for which one iteration gives convergence and run (4.6) to obtain $X_1 = U_p$. Similarly, if $2 < \kappa_2(A) \le 10$ (or a modest number $\ll u^{-1}$) then we choose r as usual from Table 3.4 but run two steps of (4.6), both of which give stable results.

4.3. Computing the Zolotarev coefficients in MATLAB. Recall that the Zolotarev coefficients $c_1, c_2, \ldots, c_{2r}$ are defined by (3.4) and (3.5). In order to obtain the c_i's, we need to first compute the complete elliptic integral K' and then compute function values of the Jacobi elliptic functions sn and cn, all for the complementary modulus $\ell' = \sqrt{1-\ell^2}$. The standard approach for these tasks is based on the arithmetic-geometric mean (AGM) method; see, e.g., [1, Ch. 16 and 17]. MATLAB provides the functions `ellipke` (for the computation of complete ellptic integrals) and `ellipj` (for the computation of function values of the Jacobi elliptic functions), which are based on the AGM method. Unfortunatley, the functions `ellipke` and `ellipj` use the complementary parameter $m' = (\ell')^2$ as input. Moreover, `ellipke` gives inaccurate values for K' for values of m' close to 1.

For our application, we have $\ell = \frac{1}{\kappa_2(A)}$ and thus

$$m' = 1 - \ell^2 = 1 - \frac{1}{\big(\kappa_2(A)\big)^2}.$$

This means that, as $\kappa_2(A)$ increases, m' is indeed close to 1. Even worse, in double-precision floating-point arithmetic, m' gets rounded to 1 for $\kappa_2(A) \gtrsim 10^8$. Due to these issues, we cannot use the functions `ellipke` and `ellipj` in the form provided in MATLAB.

Fortunately, it turns out that running the AGM method requires only the value of $\sqrt{1-m'}$, but not the value of m'. Note that

$$\sqrt{1-m'} = \sqrt{1-(\ell')^2} = \ell.$$

We modified both `ellipke` and `ellipj` so that they use ℓ as their input, rather than m'. Furthermore, employing an asymptotic expansion of K' for $m' \to 1$ (or, equivalenlty, $\ell \to 0$) given in [11], we fixed the function `ellipke` so that it computes K' accurately even when ℓ is close to 0. For our actual computations of the Zolotarev coefficients $c_1, c_2, \ldots, c_{2r}$, we employ these modified versions of `ellipke` and `ellipj`.

We remark that previous attempts exist to compute the Jacobi elliptic functions reliably; see [19, 24, 28].

Finally, even with our improved implementation of computing the Zolotarev coefficients, when $1/\ell$ and r are large, rounding errors prevent the coefficients from being computed accurately, resulting in a computed Zolotarev function that does not approximate the sign function to the desired accuracy. As discussed before, we resolve this issue by allowing for two steps, which reduce r sufficiently so that the elliptic functions are computed accurately enough for our purpose. Indeed, using the MATLAB functions the blue plots in Figure 3.3 stagnate at a much higher value.

One may conceive that another solution is to use higher precision arithmetic just for computing the coefficients c_j. This does not involve matrices, so the extra cost for this is negligible when the matrix is large. However, this generally does not solve the instability because relative accuracy is lost when dealing with the terms $x^2 + c_{2j-1}$.

4.4. Stopping criterion. Although in exact arithmetic our algorithm converges in two steps, it is nontrivial to confirm that the iterate X_2 has indeed converged. One approach is to observe that for an iterate x_k whose rate of convergence is r, once we have $\|x_k - x_{k-1}\|/\|x_k\| \lesssim \epsilon^{1/r}$ we can expect $\|x_{k+1} - x_k\|/\|x_{k+1}\| \lesssim \epsilon$, that is, convergence to tolerance ϵ is achieved at x_k. More detailed arguments are available in [20, Sec. 4.9.2] for a quadratically convergent iterate and in [31] for a cubically convergent iterate.

Since the iterate we propose converges with rate $2r + 1$, this suggests that we accept X_2 as converged if

$$\frac{\|X_2 - X_1\|_F}{\|X_2\|_F} \leq u^{1/(2r+1)}. \tag{4.7}$$

In all our experiments (4.7) was always satisfied. Another, more expensive but perhaps more reliable, way to test convergence is to check that $\frac{\|X_2^* X_2 - I\|_F}{\sqrt{n}}$ is $\mathcal{O}(u)$.

Although (4.7) was satisfied in all our experiments, it may fail to hold in unlucky cases, for example when poor estimates of α, ℓ_0 are used so that $\alpha \ll \|A\|_2$ or $\ell_0 \gg \sigma_{\min}(X_0)$. When this happens we suggest running Zolo-pd again on X_2 (not A). Although X_2 may not be a numerically orthogonal matrix its singular values are still mapped to values close to 1, so $\kappa_2(X_2) \ll \kappa_2(A)$. In particular if $\kappa_2(X_2) \leq 2$ then Zolo-pd gives single-step convergence via the Cholesky-based implementation as discussed in section 4.2.

5. Overall algorithms. Putting it all together, we summarize the three algorithms that we propose: Zolo-pd for the polar decomposition, Zolo-eig for the symmetric eigenvalue decomposition, and Zolo-SVD for the SVD.

5.1. Pseudocodes. Algorithm 5.1 is the pseudocode for Zolo-pd. Note that it is shown explicitly as a two-step algorithm without iterations. As noted in section 4.2, for well-conditioned A ($\kappa_2(A) \leq 2$) we can skip the first iteration of (5.1) and just run (5.2) by choosing r that gives a single-step convergence. Furthermore, since $\kappa_2(A) = \mathcal{O}(1)$ we can safely invoke the Cholesky-based implementation in Section 4.2, so the algorithm becomes more than twice faster than when $\kappa_2(A) > 100$.

Algorithm 5.1 Zolo-pd: compute the polar decomposition $A = U_pH$

1: Estimate $\alpha \gtrsim \sigma_{\max}(A), \beta \lesssim \sigma_{\min}(A)$, $X_0 = A/\alpha$, $\ell = \beta/\alpha$.
2: Choose r based on $\kappa = 1/\ell$ from Figure 3.4. If $\kappa < 2$ then $X_1 = A$ and skip to (iv).
3: Compute X_1 and X_2:
  (i). Compute c_j as in (3.3) such that $R(x)$ is the type $(2r+1, 2r)$ best rational approximate to $\mathrm{sign}(x)$ on the interval $[\ell, 1]$.
  (ii). Compute X_1 by

$$\left\{\begin{aligned} \begin{bmatrix} X_0 \\ \sqrt{c_{2j-1}}I \end{bmatrix} &= \begin{bmatrix} Q_{j1} \\ Q_{j2} \end{bmatrix} R, \quad j = 1, \ldots, r, \\ X_1 &= \frac{1}{R(1)} \left(X_0 + \sum_{j=1}^{r} \frac{a_j}{\sqrt{c_{2j-1}}} Q_{j1} Q_{j2}^* \right). \end{aligned}\right. \tag{5.1}$$

  (iii). Update $\ell \leftarrow R(\ell)/R(1)$, compute c_j and $R(x)$ as in step (i) on the new interval $[\ell, 1]$.
  (iv). Compute X_2 by

$$\left\{\begin{aligned} Z_{2j-1} &= X_1^* X_1 + c_{2j-1} I, \quad W_{2j-1} = \mathrm{Chol}(Z_{2j-1}), \\ X_2 &= \tfrac{1}{R(1)} \left(X_1 + \textstyle\sum_{j=1}^{r} a_j (X_2 W_{2j-1}^{-1}) W_{2j-1}^{-*} \right). \end{aligned}\right. \tag{5.2}$$

  Verify that the conditions (4.7) hold.
4: $U_p = X_2$, $H = \frac{1}{2}(U_p^* A + (U_p^* A)^*)$.

As mentioned in the introduction, Zolo-eig (Algorithm 5.2) and Zolo-SVD (Algorithm 5.3) use the framework as the QDWH-based algorithms in [30] but replaces QDWH with Zolo-pd for the part that computes the polar decomposition.

Algorithm 5.2 Zolo-eig: computes an eigendecomposition of a symmetric (Hermitian) matrix A

1: Choose σ, estimate of the median of $\mathrm{eig}(A)$
2: Compute polar factor U_p of $A - \sigma I = U_pH$ by Zolo-pd
3: Compute $V_1 \in \mathbb{C}^{n\times k}$ such that $\frac{1}{2}(U_p + I) = V_1V_1^*$ via subspace iteration, then form a unitary matrix $V = [V_1\ V_2]$
4: Compute $A_1 = V_1^*AV_1$ and $A_2 = V_2^*AV_2$
5: Repeat steps 1–4 with $A := A_1, A_2$ until A is diagonalized

Algorithm 5.3 Zolo-SVD: compute the SVD of a general matrix A

1: Compute the polar decomposition $A = U_pH$ via Zolo-pd
2: Compute the symmetric eigendecomposition $H = V\Sigma V^*$ via Zolo-eig
3: Form $U = U_pV$. $A = U\Sigma V^*$ is the SVD

5.2. Cost comparison. Here we compare the computational cost of our Zolotarev-based algorithms with the standard algorithms.

Polar decomposition. Table 5.1 compares Zolo-pd with QDWH and the scaled Newton iteration [20, Ch. 8], the two most practical algorithms for the unitary polar factor of $A \in \mathbb{C}^{m\times n}$ (we need $m = n$ for the scaled Newton iteration as it is applicable only to nonsingular matrices). It summarizes the backward stability, the dominant type of operation, the maximum iteration count and arithmetic cost in flops required for $\kappa_2(A) \le 10^{16}$; for well-conditioned matrices the flop count generally decreases. The arithmetic cost for QDWH is taken from the flop count in [33], and we can also derive that of Zolo-pd similarly. The parenthesized entry at the bottom of the table shows the arithmetic cost along the critical path when the r QR and Cholesky factorizations in (5.1), (5.2) are computed in parallel. The arithmetic cost of the scaled Newton iteration assumes that matrix inverses are computed in the standard way based on LU factorization with partial pivoting.

Zolo-pd requires more arithmetic cost than QDWH and scaled Newton, by about a factor 3. However, along the critical path it requires the fewest flops, so in a parallel implementation we expect Zolo-pd to be the fastest.

TABLE 5.1
Comparison of algorithms for the polar decomposition.

	Zolo-pd	QDWH	scaled Newton
Backward stability	$(\surd)$	$\surd$	$\surd^a$
Dominant operation	QR	QR	inversion
Max. # iterations	2	6	9
Arithmetic cost	$64mn^2 + \frac{8}{3}n^3$	$22mn^2 + \frac{4}{3}n^3$	$18n^3$
	$(8mn^2 + \frac{1}{3}n^3)$		

[a]Matrix inverses need to be computed in a mixed backward-forward stable manner to prove backward stability of scaled Newton [10, 32]. Using the standard method of LU with partial pivoting for inversion this condition is not guaranteed, and it can be indeed unstable [32]. The parenthesized $(\surd)$ means the stability is observed numerically but not yet established theoretically.

Symmetric eigendecomposition. Table 5.2 compares the spectra-divide-and-conquer algorithms Zolo-eig, QDWH-eig, IRS (implicit repeated squaring [5]), and ZZY [43], along with the standard algorithm that performs tridiagonalization followed by the symmetric tridiagonal QR algorithm [15, § 8.3],[35, Ch. 8]. The algorithms compute both the eigenvalues and eigenvectors. In addition to the information shown in Table 5.1, Table 5.2 shows whether the algorithm minimizes communication in the asymptotic sense.

Following [33], the arithmetic cost of QDWH-eig and Zolo-eig is obtained assuming that the splitting points σ are chosen such that $\kappa_2(A - \sigma I) \le 10^5$, for which $r = 5$ is sufficient as discussed in Section 3.5; we can take a different σ if this does not hold. Note that the arithmetic cost along the critical path of Zolo-eig in a parallel implementation is about the same as that of the standard algorithm.

SVD. Table 5.3 compares four SVD algorithms: Zolo-SVD, QDWH-SVD, IRS, and the standard algorithm that performs bidiagonalization followed by bidiagonal QR [15, § 8.6]. The arithmetic cost shows the flop counts for a square $n \times n$ matrix A, and since for Zolo-SVD and QDWH-SVD it depends on the condition number $\kappa_2(A)$, we show the arithmetic cost in the range $\kappa_2(A) = 1.1$–10^{16}.

The arithmetic cost along the critical path of Zolo-SVD is slightly lower than that of the standard algorithm.

Table 5.2
Comparison of algorithms for symmetric eigendecomposition.

	Zolo-eig	QDWH-eig	IRS [5]	ZZY [43]	standard
Min. communication?	$\surd$	$\surd$	$\surd$	$\times$	$\times$
Backward stability	$(\surd)$	$\surd$	conditional	$(\surd)$	$\surd$
Max. # iterations	2	6	53	53	
Arithmetic cost	$39.6n^3$ $(10.25n^3)$	$27n^3$	$\approx 720n^3$	$\approx 370n^3$	$9n^3$

Table 5.3
Comparison of algorithms for the SVD.

	Zolo-SVD	QDWH-SVD	IRS	standard
Min. communication?	$\surd$	$\surd$	$\surd$	$\times$
Backward stability	$(\surd)$	$\surd$	conditional	$\surd$
Max. # iterations	2	6	53	
Arithmetic cost ($m = n$)	$48n^3$–$111n^3$ $(18.5n^3$–$23.5n^3)$	$35n^3$–$52n^3$	$\approx 5700n^3$	$26n^3$

5.3. Backward stability. As mentioned in the introduction, the backward stability of Zolo-eig and Zolo-SVD rests on that of Zolo-pd for the polar decomposition. For iterations for the polar decomposition, backward stability analysis is given in [32], which shows that the computed polar decomposition is backward stable if two conditions are satisfied: (i) Each iterate is backward-forward stable, that is, the computed approximant $\widehat{Y}$ to $Y = f(X)$ satisfies $\widehat{Y} = f(\widetilde{X}) + \epsilon\|\widehat{Y}\|_2$ where $\widetilde{X} = \widehat{X} + \epsilon\|\widehat{X}\|_2$, where ϵ denotes a matrix whose norm is $\mathcal{O}(u)$. (ii) The function $f(x)$ lies above $y = x$.

Of the two conditions, the second is more nonintuitive and indeed gives insights into some unstable iterations proposed in the literature. QDWH satisfies the two conditions and hence is backward stable if pivoting (row and column) is used for computing the QR factorizations.

For Zolo-pd, it is easy to verify that the second condition is satisfied, because the mapping function $f(x) = \hat{Z}_{2r+1}(x;\ell_i)$ is the best approximant to the sign function, and $y = x$ can be regarded as a member of $(2r+1, 2r)$ rational functions. However, regarding the first condition, the presence of r QR factorizations seems to make the discussion nontrivial. Although experiments demonstrate the excellent backward stability of Zolo-pd, its proof therefore remains an open problem.

5.4. Other implementation details. As in [33], we perform a Newton–Schulz postprocessing after computing the orthogonal factors (matrices of singular vectors and eigenvectors), which improves the orthogonality and backward stability of the computed results. For computing the shifts σ in QDWH-eig we adopted the method in [33] of taking the median of the diagonal elements.

Zolo-SVD is also able to compute the SVD for rank-deficient matrices, as described in [33]. Other implementation issues, including taking an initial QR factorization when m is much larger than n, executing subspace iteration and estimating $\sigma_{\max}(A)$ and $\sigma_{\min}(A)$, are the same as in the QDWH-based algorithms, and we refer to [33] for details. Note that two-step convergence is attained as long as $\alpha > \sigma_{\max}(A)$ and $\ell < \sigma_{\min}(A/\alpha)$, so "safe" estimates that satisfy these are preferred.

6. Numerical experiments. We present numerical experiments to examine the performance of Zolo-pd, Zolo-eig and Zolo-SVD, and to compare them with the QDWH-based algorithms and standard algorithms. The experiments here are all sequential: in particular, the r QR factorizations are not computed independently, and nor is a communication-minimizing implementation used. These will be tested in future work.

All the experiments were carried out in MATLAB version R2013a on a machine with an Intel Xeon processor with eight cores and sixteen threads, and 64GB RAM, using IEEE double precision arithmetic.

6.1. Polar decomposition. We first compare Zolo-pd with the two most practical iterations among the existing algorithms: QDWH and the scaled Newton iteration [20, p. 205] with the scaling due to Byers and Xu [10], shown in Table 6.1 as "Newton". We generate n-by-n matrices with $n = 20000$ by forming $A = U\Sigma V^*$, where U, V are random orthogonal matrices and Σ is a diagonal matrix of singular values, which form an arithmetic sequence (the distribution of singular values has little effect on the performance). Table 6.1 shows the iteration counts "iter", backward error $\|\widehat{U}_p\widehat{H} - A\|_F/\|A\|_F$ "berr", orthogonality measure $\|\widehat{U}_p^*\widehat{U}_p - I\|_F/\sqrt{n}$ "orth", and the runtime in seconds. The numbers in parentheses for Zolo-pd in the "iter" row show the degree r of the polynomials $P(x), Q(x)$, and those in "time" are the runtime of Zolo-pd along the critical path, that is, assuming the r independent terms in (5.1) and (5.2) are computed in parallel, it counts only the runtime of the one that took the longest among the r QR (or Cholesky) factorizations in (5.1) and (5.2).

TABLE 6.1
Performance comparison of polar decomposition algorithms, $A \in \mathbb{R}^{20000\times 20000}$.

$\kappa_2(A)$		1.1	1.5	10	10^5	10^{10}	10^{15}
iter	Zolo-pd	1 (4)	1 (6)	2 (3)	2 (5)	2 (7)	2 (8)
	QDWH	3	3	4	5	6	6
	Newton	4	5	6	8	8	9
berr	Zolo-pd	1.6e-15	2.1e-15	1.5e-15	1.6e-15	1.7e-15	2.1e-15
	QDWH	1.1e-15	1.2e-15	1.2e-15	1.5e-15	1.4e-15	1.4e-15
	Newton	2.4e-13	2.5e-13	2.5e-13	2.5e-13	2.4e-13	2.4e-13
orth	Zolo-pd	1.5e-15	2.0e-15	1.1e-15	1.0e-15	1.1e-15	1.7e-15
	QDWH	7.7e-16	1.1e-15	8.9e-16	1.1e-15	7.6e-16	1.1e-15
	Newton	1.7e-13	1.7e-13	1.7e-13	1.7e-13	1.7e-13	1.7e-13
time	Zolo-pd	475 (164)	682 (164)	680 (267)	1604 (369)	2249 (373)	2539 (370)
	QDWH	353	355	448	659	877	878
	Newton	343	418	483	626	629	706

We observe the following.

- As predicted by the theory, Zolo-pd requires just two iterations for convergence. The number of iterations for the other two methods also accurately reflect the theory, see [10] and [20, p. 206] for scaled Newton and [31] for QDWH.
- For large $\kappa_2(A)$, the runtime of Zolo-pd becomes much longer than those of the other two methods. This is because r becomes large and hence many QR factorizations are needed per iteration, which are computed sequentially here. However, along the critical path, its runtime is much shorter, and independent of r for $\kappa_2(A) \geq 10^2$ (in which case the critical path is essentially one QR and one Cholesky).
- Zolo-pd and QDWH give excellent backward error and orthogonality measure. Those of scaled Newton are about two orders of magnitude larger.

6.2. Symmetric eigendecomposition.

6.2.1. Spectral divide-and-conquer algorithms. We first compare spectral divide-and-conquer algorithms: Zolo-eig, QDWH-eig, the general algorithm applicable to generalized eigenproblems due to Ballard, Demmel and Dumitriu [5], which we call IRS (Implicit Repeated Squaring), and the algorithm QUAD in [43], which we call ZZY. These methods can be implemented in a communication-minimizing manner.

We set the matrix size to $n = 100$ and generate symmetric matrices $A = V\Lambda V^T$, where V is a random orthogonal matrix and $\Lambda = \mathrm{diag}(1, r, r^2, \dots, r^{n-1})$ with $r = -\kappa^{-1/(n-1)}$, in which $\kappa = \kappa_2(A)$ is the prescribed condition number, which we set to $10^2, 10^5$ and 10^{15}. The eigenvalue of A closest to 0 is κ^{-1}.

Here we consider computing an invariant subspace V_1 corresponding to the positive eigenvalues of A. To do so we apply one recursion of Zolo-eig (steps 1–4 of Algorithm 5.2) and QDWH-eig on A.

We generated 100 matrices for each case $\kappa = 10^2, 10^8, 10^{15}$, and show in Table 6.2 the maximum and minimum values of the iteration counts, shown as "iter", along with the backward error $\|E\|_F/\|A\|_F$ where $[\widehat{V}_1\ \widehat{V}_2]^* A [\widehat{V}_1\ \widehat{V}_2] = \left[\begin{smallmatrix} A_1 & E^* \\ E & A_2 \end{smallmatrix}\right]$, shown as "berr". The orthogonality measure $\|\widehat{V}_1^* \widehat{V}_1 - I_k\|_F/\sqrt{n}$ was $\mathcal{O}(u)$ for all the methods.

TABLE 6.2
Iteration count and residual of spectral divide-and-conquer algorithms.

$\kappa_2(A)$		10^2		10^8		10^{15}	
		min	max	min	max	min	max
iter	Zolo-eig	2 (3)	2 (3)	2 (6)	2 (6)	2 (8)	2 (8)
	QDWH-eig	4	5	5	5	6	6
	ZZ	12	12	32	32	55	56
	IRS	12	13	32	32	54	55
berr	Zolo-eig	5.6e-16	6.1e-16	5.8e-16	6.5e-16	6.4e-16	7.3e-16
	QDWH-eig	8.5e-16	9.4e-16	8.5e-16	9.7e-16	8.4e-16	9.8e-16
	ZZ	1.6e-15	1.9e-15	2.6e-15	2.9e-15	2.9e-15	4.1e-15
	IRS	2.1e-15	2.9e-14	2.4e-13	3.3e-12	3.8e-10	4.0e-8

Observations:

- Zolo-eig always converges in two iterations. QDWH-eig converges within six iterations, whereas ZZ and IRS need many more iterations, especially in the difficult cases where $\kappa_2(A)$ is large.
- Zolo-eig and QDWH-eig performed in a backward stable manner throughout.

This illustrates Zolo-eig and QDWH-eig are significantly superior to the other spectral divide-and-conquer algorithms that minimize communication, as also predicted by Table 5.2.

6.2.2. Comparison with conventional algorithms for the full symmetric eigendecomposition. We now compare algorithms for computing the full eigendecomposition of a symmetric matrix. We compare Zolo-eig, QDWH-eig and MATLAB's built-in function `eig`, which is based on reduction to tridiagonal form followed by the divide-and-conquer algorithm [17]. Here we generated Hermitian matrices A as follows: form a random matrix B by the MATLAB function $B =$`randn(n)`, then let $A = \frac{1}{2}(B + B^*)$. Below we report the average of three runs.

Table 6.3 shows the backward error $\|\widehat{V}\widehat{\Lambda}\widehat{V}^T - A\|_F/\|A\|_F$. While all the methods are backward stable, the backward errors of QDWH-eig and Zolo-eig are smaller than those of `eig`, by more than a factor 3.

TABLE 6.3
Backward error $\|A - \widehat{V}\widehat{\Lambda}\widehat{V}^T\|_F / \|A\|_F$.

n	4000	8000	12000	16000	20000
QDWH-eig	2.4e-15	2.8e-15	3.2e-15	3.6e-15	3.8e-15
Zolo-eig	2.4e-15	2.9e-15	3.2e-15	3.6e-15	3.8e-15
MATLAB `eig`	7.6e-15	1.0e-14	1.3e-14	1.4e-14	1.6e-14

Table 6.4 shows the orthogonality measure $\|\widehat{V}^T\widehat{V} - I\|_F/\sqrt{n}$. We see that those of Zolo-eig and QDWH-eig are much smaller than `eig`. This improvement is largely due to the Newton–Schulz postprocessing.

TABLE 6.4
Orthogonality measure of $\widehat{V}$: $\|\widehat{V}^T\widehat{V} - I\|_F/\sqrt{n}$.

n	4000	8000	12000	16000	20000
Zolo-eig	8.0e-16	8.4e-16	8.6e-16	8.8e-16	9.0e-16
QDWH-eig	8.0e-16	8.4e-16	8.6e-16	8.8e-16	9.0e-16
MATLAB `eig`	6.4e-15	8.7e-15	1.1e-14	1.2e-14	1.4e-14

The above behavior was not peculiar to this class of matrices, and was observed in all our experiments. These results suggest that the stability of Zolo-eig is comparable to QDWH-eig, and is typically better than conventional algorithms. Of course, all three algorithms are stable and the difference in backward error is a constant that is usually insignificant.

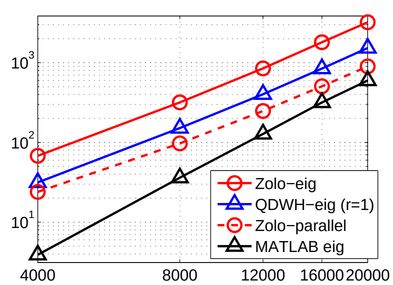

FIG. 6.1. *Eigendecomposition runtime for varying matrix size.*

Figure 6.1 shows the SVD runtime. Zolo-parallel shows the runtime of Zolo-eig along the critical path (as in Zolo-pd, accounting only for the longest of the r QR factorizations). Observe that while Zolo-eig and Zolo-parallel are slower than MATLAB's `eig`, they seem to scale slightly better as n grows.

6.3. SVD algorithms. We now turn to the SVD algorithms Zolo-SVD, QDWH-SVD and MATLAB's `svd` (based on bidiagonal reduction and divide-and-conquer [16]). We generate test matrices by forming $n \times n$ matrices $A = U\Sigma V^*$, where U, V are random orthogonal matrices and Σ is a diagonal matrix of singular values, uniformly distributed.

Varying matrix sizes. We set $\kappa_2(A) = 10^5$ and varied the matrix size n. Tables 6.5 and 6.6 show the backward error $\|A - \widehat{U}\widehat{\Sigma}\widehat{V}^T\|_F/\|A\|_F$ and orthogonality measure $\max(\|\widehat{U}^T\widehat{U} - I\|_F/\sqrt{n}, \|\widehat{V}^T\widehat{V} - I\|_F/\sqrt{n})$. The same comments as for the symmetric eigendecomposition apply: while all algorithms give acceptably small backward error and orthogonality measure, those of Zolo-SVD and QDWH-SVD are notably better than the standard algorithm MATLAB `svd`. The stability behavior is largely independent of the condition number $\kappa_2(A)$.

TABLE 6.5
Backward error for SVD $\|A - \widehat{U}\widehat{\Sigma}\widehat{V}^T\|_F/\|A\|_F$.

n	4000	8000	12000	16000	20000
Zolo-SVD	2.4e-15	2.9e-15	3.2e-15	3.6e-15	3.8e-15
QDWH-SVD	2.4e-15	2.7e-15	3.0e-15	3.3e-15	3.5e-15
MATLAB `svd`	7.9e-15	1.0e-14	1.3e-14	1.4e-14	1.6e-14

TABLE 6.6
Orthogonality of computed $\widehat{U}, \widehat{V}$*:* $\max(\|\widehat{U}^T\widehat{U} - I\|_F/\sqrt{n}, \|\widehat{V}^T\widehat{V} - I\|_F/\sqrt{n})$.

n	4000	8000	12000	16000	20000
Zolo-SVD	8.1e-16	8.4e-16	8.6e-16	8.8e-16	9.0e-16
QDWH-SVD	8.1e-16	8.4e-16	8.6e-16	8.8e-16	9.0e-16
MATLAB `svd`	7.4e-15	9.7e-15	1.2e-14	1.4e-14	1.5e-14

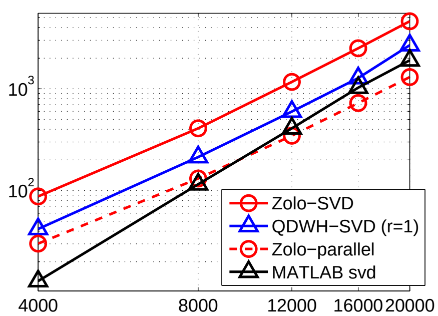

$\kappa_2(A) = 1.5$.

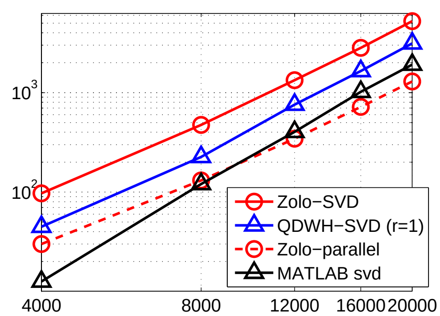

$\kappa_2(A) = 10^5$.

FIG. 6.2. *SVD runtime for varying matrix size.*

Figure 6.2 shows the SVD runtime for varying matrix size, and $\kappa_2(A) = \{1.5, 10^5\}$. As before Zolo-parallel shows the runtime of Zolo-SVD along the critical path. Zolo-SVD and Zolo-parallel scale slightly better than MATLAB's `svd` as n grows, and for $n \geq 10000$ Zolo-parallel appears to become faster when A is well-conditioned, suggesting that Zolo-SVD can outperform a standard SVD algorithm with an optimized implementation.

A big bulk of the runtime of a standard, reduction-based algorithm is consumed in the reduction step [42] (to tridiagonal or bidiagonal form), which becomes a communication bottleneck in a parallel implementation. Spectral divide-and-conquer algorithms overcome this issue by bypassing the reduction and always working with the whole matrix.

The above experiments are only with square nonsingular matrices, but all the algorithms are applicable to rectangular and rank-deficient matrices. Indeed, the experiments in [33] illustrate that QDWH-eig tends to compute the rank of rank-deficient matrices or small singular values more accurately, and we observed the same behavior with Zolo-SVD.

6.4. Summary of numerical experiments. The results of our experiments can be summarized as follows.

- Zolo-type ($r \geq 1$) algorithms have excellent numerical backward stability, comparable to that of QDWH-type ($r = 1$).
- Zolo-type and QDWH-type algorithms are generally much faster and more stable than other spectral divide-and-conquer algorithms.
- On a sequential implementation, MATLAB's functions `eig` and `svd` employing divide-and-conquer following reduction to tridiagonal or bidiagonal was the fastest, both for the eigendecomposition and the SVD. However, Zolo-eig and Zolo-svd are predicted to have competitive speed when implemented in parallel.

On massively parallel computing architectures where the communication cost dominates arithmetic cost, it is expected that the high parallelizability and excellent stability of Zolo-type algorithms provide an attractive alternative to the standard ones.

7. Discussion. Zolo-pd is a matrix iteration that draws heavily from rational approximation theory. Rational approximation, in turn, is closely related to numerical contour integration in the complex plane: Hale, Higham and Trefethen [19] propose an algorithm for computing matrix functions via numerical contour integration combined with conformal mapping to improve the region of analyticity, and they show that numerical contour integration can be regarded as a rational approximation, see also [38]. In particular, when the function is $\sqrt{x}$, their contour integration algorithm becomes closely related to Zolotarev's rational approximation to the square root (obtained by $\frac{P_r(x)}{Q_r(x)} \approx \sqrt{x}$, where $Z_{2r+1}(x;\ell) = x\frac{P_r(x^2)}{Q_r(x^2)} \approx \mathrm{sign}(x)$ is the Zolotarev function for the sign function), applicable for computing $A^{1/2}$ for a matrix with positive eigenvalues. We can adjust this approach for the sign function to compute the unitary polar factor U_p of A. This results in a type $(2r+1, 2r)$ approximant

$$U_p \approx A + \sum_{j=1}^{r} a_j A(A^*A + c_{2j-1}I)^{-1}, \tag{7.1}$$

where a_j, c_{2j-1} are the same as in (4.5). This is essentially the first iteration of Zolo-pd.

Compared with this contour integral-based derivation of (7.1), our algorithm Zolo-pd makes three improvements. First, by using the QR factorization to avoid matrix inversions for computing matrices of the form $X(X^*X+c_{2i-1}I)^{-1}$, we improve the numerical stability significantly: a direct implementation of (7.1) (or one using Cholesky factorization as in (4.6)) gives poor stability when $\kappa_2(A) \gg 1$. Second, by allowing the algorithm to iterate two steps, we reduce the arithmetic cost dramatically (from $r > 140$ once to $r = 8$ twice). Finally, Zolo-pd resolves the numerical instability when r is large, observed in Section 3.4.

We note that the idea of allowing for the second step is highly nontrivial from the viewpoint of contour integration (or its relation to rational approximation), whereas our derivation of Zolo-pd as an iterative algorithm for the polar decomposition makes it just natural.

Acknowledgments. We would like to thank Stefan Güttel, Nick Higham, Françoise Tisseur, and Nick Trefethen for their valuable suggestions and comments.

REFERENCES

[1] M. Abramowitz and I. A. Stegun. *Handbook of Mathematical Functions.* Dover, Mineola, NY, 1965.

[2] N. I. Akhiezer. *Elements of the Theory of Elliptic Functions.* AMS, Providence, RI, 1990.

[3] N. I. Akhiezer. *Theory of Approximation.* Dover, Mineola, NY, 1992.

[4] Z. Bai, J. Demmel, J. Dongarra, A. Ruhe, and H. van der Vorst. *Templates for the Solution of Algebraic Eigenvalue Problems: A Practical Guide.* SIAM, Philadelphia, PA, 2000.

[5] G. Ballard, J. Demmel, and I. Dumitriu. Minimizing communication for eigenproblems and the singular value decomposition. Technical Report 237, LAPACK Working Note, 2010.

[6] G. Ballard, J. Demmel, O. Holtz, and O. Schwartz. Minimizing communication in numerical linear algebra. *SIAM J. Matrix Anal. Appl.*, 32(3):866–901, 2011.

[7] G. Ballard, J. Demmel, and N. Knight. Avoiding communication in successive band reduction. Technical Report UCB/EECS-2013-131, EECS Department, University of California, Berkeley, Jul 2013.

[8] B. Beckermann. Optimally scaled Newton iterations for the matrix square root. Presentation at the FUN13 workshop on “Advances in Matrix Functions and Matrix Equations”, Manchester, United Kingdom, 2013.

[9] D. Braess. On rational approximation of the exponential and the square root function. In P. R. Graves-Morris, E. B. Saff, and R. S. Varga, editors, *Rational Approximation and Interpolation*, volume 1105 of *Lecture Notes in Mathematics*, pages 89–99, 1984.

[10] R. Byers and H. Xu. A new scaling for Newton's iteration for the polar decomposition and its backward stability. *SIAM J. Matrix Anal. Appl.*, 30:822–843, 2008.

[11] B. C. Carlson and J. L. Gustafson. Asymptotic expansion of the first elliptic integral. *SIAM J. Math. Anal.*, 16(5):1072–1092, 1985.

[12] V. Druskin, S. Güttel, and L. Knizhnerman. Near-optimal perfectly matched layers for indefinite helmholtz problems. MIMS EPrint, Manchester Institute for Mathematical Sciences, The University of Manchester, UK, 2013.

[13] A. George and K. Ikramov. Is the polar decomposition finitely computable? *SIAM J. Matrix Anal. Appl.*, 17:348–354, 1996.

[14] A. George and K. Ikramov. Addendum: Is the polar decomposition finitely computable? *SIAM J. Matrix Anal. Appl.*, 18:264, 1997.

[15] G. H. Golub and C. F. Van Loan. *Matrix Computations.* The Johns Hopkins University Press, Baltimore, MD, 4th edition, 2012.

[16] M. Gu and S. C. Eisenstat. A divide-and-conquer algorithm for the bidiagonal SVD. *SIAM J. Matrix Anal. Appl.*, 16(1):79–92, 1995.

[17] M. Gu and S. C. Eisenstat. A divide-and-conquer algorithm for the symmetrical tridiagonal eigenproblem. *SIAM J. Matrix Anal. Appl.*, 16(1):172–191, 1995.

[18] S. Güttel, E. Polizzi, P. Tang, and G. Viaud. Zolotarev quadrature rules and load balancing for the FEAST eigensolver. MIMS EPrint 2014.39, Manchester Institute for Mathematical Sciences, The University of Manchester, UK, 2014.

[19] N. Hale, N. J. Higham, and L. N. Trefethen. Computing A^α, $\log(A)$, and related matrix functions by contour integrals. *SIAM J. Numer. Anal.*, 46(5):2505–2523, 2008.

[20] N. J. Higham. *Functions of Matrices: Theory and Computation.* SIAM, Philadelphia, PA, 2008.

[21] N. J. Higham and P. Papadimitriou. A parallel algorithm for computing the polar decomposition. *Parallel Comput.*, 20:1161–1173, 1994.

[22] R. A. Horn and C. R. Johnson. *Matrix Analysis.* Cambridge University Press, second edition, 2012.

[23] B. Iannazzo. The geometric mean of two matrices from a computational viewpoint. *arXiv:1201.0101*, 2011.

[24] A. D. Kennedy. Fast evaluation of Zolotarev coefficients. In *Proceedings of the Third International Workshop on Numerical Analysis and Lattice QCD*, pages 169–189, 2003.

[25] A. D. Kennedy. Approximation theory for matrices. *Nucl. Phys. B–Proc. Sup.*, 128:107–116, 2004.

[26] C. Kenney and A. Laub. A hyperbolic tangent identity and the geometry of padé sign function iterations. *Numer. Algorithms*, 7:111–128, 1994. 10.1007/BF02140677.

[27] C. Kenney and A. Laub. The matrix sign function. *IEEE Trans. Automat. Control*, 40(8):1330–

1348, 1995.
[28] B. Laszkiewicz and K. Zietak. Numerical experiments with algorithms for the ADI and Zolotarev coefficients. *Appl. Math. Comput.*, 206(1):298–312, 2008.
[29] A. A. Medovikov and V. I. Lebedevt. Variable time steps optimization of L_ω-stable Crank-Nicolson method. *Russ. J. Numer. Anal. Math. Modelling*, 20(3):283–303, 2005.
[30] Y. Nakatsukasa. *Algorithms and Perturbation Theory for Matrix Eigenvalue Problems and the Singular Value Decomposition.* PhD thesis, University of California, Davis, 2011.
[31] Y. Nakatsukasa, Z. Bai, and F. Gygi. Optimizing Halley's iteration for computing the matrix polar decomposition. *SIAM J. Matrix Anal. Appl.*, 31(5):2700–2720, 2010.
[32] Y. Nakatsukasa and N. J. Higham. Backward stability of iterations for computing the polar decomposition. *SIAM J. Matrix Anal. Appl.*, 33(2):460–479, 2012.
[33] Y. Nakatsukasa and N. J. Higham. Stable and efficient spectral divide and conquer algorithms for the symmetric eigenvalue decomposition and the SVD. *SIAM J. Sci. Comp*, 35(3):A1325–A1349, 2013.
[34] I. Ninomiya. Best rational starting approximations and improved Newton iteration for the square root. *Math. Comp.*, 24(110):391–404, 1970.
[35] B. N. Parlett. *The Symmetric Eigenvalue Problem.* SIAM, Philadelphia, PA, 1998.
[36] P. P. Petrushev and V. A. Popov. *Rational Approximation of Real Functions.* Cambridge University Press, Cambridge, United Kingdom, 2011.
[37] M. J. D. Powell. *Approximation Theory and Methods.* Cambridge University Press, Cambridge, United Kingdom, 1981.
[38] L. N. Trefethen, J. A. C. Weideman, and T. Schmelzer. Talbot quadratures and rational approximations. *BIT*, 46(3):653–670, 2006.
[39] L. N. Trefethen. *Approximation Theory and Approximation Practice.* SIAM, Philadelphia, PA, 2013.
[40] J. van den Eshof. *Nested Iteration Methods for Nonlinear Matrix Problems.* PhD thesis, Proefschrift Universiteit Utrecht, 2003.
[41] J. van den Eshof, T. Lippert, A. Frommer, K. Schilling, and H. van der Vorst. Numerical methods for the QCD overlap operator: I. sign-function and error bounds. *Comput. Phys. Comm.*, 146:203–224, 2002.
[42] F. G. V. Zee, R. van de Geijn, and G. Quintana-Orti. Restructuring the tridiagonal and bidiagonal QR algorithm for performance. *ACM Trans. Math. Soft.*, 40(3):18:1–18:34, 2014.
[43] Z. Zhang, H. Zha, and W. Ying. Fast parallelizable methods for computing invariant subspaces of Hermitian matrices. *J. Comput. Math.*, 25(5):583–594, 2007.
[44] E. I. Zolotarev. Application of elliptic functions to questions of functions deviating least and most from zero. *Zap. Imp. Akad. Nauk. St. Petersburg,*, 30(5), 1877. Reprinted in his *Collected Works*, Vol. II, Izdat. Akad. Nauk SSSR, Moscow, 1932, pp. 1–59. In Russian.